amt-2017-194

The CHRONOS mission: Capability for sub-hourly synoptic observations of carbon monoxide and methane to quantify emissions and transport of air pollution

David P. Edwards, Helen M. Worden, Doreen Neil, Gene Francis, Tim Valle, and Avelino F. Arellano Jr.

Response to Reviewer 1:

We thank the reviewer for their careful evaluation of our manuscript. We address each comment (in blue) with an embedded response (in black) below. We detail new text that has been added to the revised manuscript (in green).

General Comments:

CO2 and CH4 monitoring with gas filter correlation technology from GEO is very important mission from both global warming and air quality monitoring points of view. Observation needs are well described. Recently many GEO and LEO GHG monitoring programs have been proposed. The authors should describe difference from the Geo-CARB program using grating spectrometer technology.

We agree that more description of the differences between CHRONOS and GeoCARB, which was recently selected for the NASA EVM-2 program, is needed. We have added the following text to Section 6.1:

NASA selected the GeoCARB mission in November 2016, with capability to measure CO in one spectral region (Polonsky et al. 2014; Kumer et al., 2013) and primary carbon cycle science objectives unrelated to air pollution transport. Compared to the CHRONOS requirement for CO measurement in two spectral regions, this GeoCARB limitation to CO in one spectral region precludes GeoCARB from evaluating vertical pollution transport, or providing the test of these atmospheric motions as calculated by models (NAS, 2017). Both Polonsky et al. (2104) and Kumer et al. (2013) describe mission descopes that eliminate GeoCARB measurements of CO entirely if needed to ensure success for GeoCARB CO_2 and solar induced fluorescence science objectives.

And to Section 6.2:

GeoCARB describes CH_4 measurements in the SWIR (2.3 μm) region with 1% precision three times per day at 5 km x 5 km spatial resolution (O'Brien et al., 2016), although earlier studies (Kumer et al., 2013) explored methane measurements at 1.65 μm. GeoCARB's more frequent methane observations than TROPOMI may provide for similar precision in a smaller spatial footprint than TROPOMI. CHRONOS could observe CH_4 as often as every 10 minutes in daylight with 0.7% precision and 4 km x 4 km resolution. These frequent CHRONOS CH_4 measurements could be co-added to improve hourly precision, or used to examine anthropogenic source evolution over time.

GeoCARB parameters are also included in Table 3, now revised in response to Reviewer 2.

CHRONOS has advantage to measure both solar reflected light from surface and thermal radiation from middle of the troposphere. However, it is not clear gas filter correlation technique is more accurate and/or precise than other technique such as grating spectrometer and FTS in CH4 retrieval.

The gas filter correlation technique achieves accuracy and precision in trace gas retrieval similar to grating spectrometers and FTS by virtue of very high effective spectral resolution and high throughput (low noise). We have clarified the choice of spectral technique by adding to the discussion in Section 3.1:

The effective spectral resolution of the GFCR response function (Edwards et al., 1999, figure 3) matches the pressure-broadened Lorentz full-width-half-maximum (FWHM) for weak-absorption lines (Beer, 1992), and ranges from 0.08 cm^{-1} to 0.16 cm^{-1} for 200 hPa to 800 hPa GFCR gas cells (Pan et al., 1995). This optimal spectral resolution for measuring tropospheric trace gas absorption and for probing the spectral line profile to obtain information on the trace gas atmospheric vertical distribution is difficult to achieve for most spectrometers without sacrificing signal amplitude (grating spectrometers) or increasing noise (Fourier transform spectrometers). The limitation for the GFCR technique is that atmospheric retrievals are made only for those gases contained within the cells of the instrument. However, for observations of CO and CH_4 from GEO (50 times farther from Earth than LEO), the advantages of both fine spectral resolution and high throughput provided by CRONOS's gas filter correlation radiometry make for a particularly robust measurement approach.

New references:

Polonsky, I. N., O'Brien, D. M., Kumer, J. B. and O'Dell, C. W.: Performance of a geostationary mission, geoCARB, to measure CO2, CH4 and CO column-averaged concentrations. Atmospheric Measurement Techniques, 7(4), pp.959-981, 2014.

Kumer, J.J.B., Rairden, R.L., Roche, A.E., Chevallier, F., Rayner, P.J. and Moore, B.: September. Progress in development of Tropospheric Infrared Mapping Spectrometers (TIMS): GeoCARB Greenhouse Gas (GHG) application. In Infrared Remote Sensing and Instrumentation XXI (Vol. 8867, p. 88670K). International Society for Optics and Photonics, 2013.

National Academies of Sciences, Engineering, and Medicine: Powering Science: NASA's Large Strategic Science Missions. Washington, DC: The National Academies Press. https://doi.org/10.17226/24857, p33, p81, 2017.

O'Brien, D. M., Polonsky, I. N., Utembe, S. R., and Rayner, P. J.: Potential of a geostationary geoCARB mission to estimate surface emissions of CO_2, CH_4 and CO in a polluted urban environment: case study Shanghai, Atmospheric Measurement Techniques, 9, 4633–4654, https://doi.org/10.5194/amt-9-4633-2016, 2016.

Pan, L., Edwards, D. P., Gille, J. C., Smith, M. W., and Drummond, J. R.: Satellite remote sensing of tropospheric CO and CH4: forward model studies of the MOPITT instrument, *Appl. Opt.*, *34*(30), 6976–6988, doi:10.1364/AO.34.006976, 1995.

Beer, R.: Remote Sensing by Fourier Transform Spectrometry, *Wiley, New York*, 1992.

How to achieve 1% accuracy in CH4 retrieval under aerosol and high thin cloud condition without light path modification information should be described in more detail.

For the retrieval of CH_4 in the presence of clouds and aerosols, we added to Section 3.2:

SCIAMACHY and GOSAT CH_4 SWIR retrievals are sensitive to scattering by dust, aerosols and thin cirrus (Gloudemans et al., 2008; Schepers et al., 2012) and address these errors by using CO_2 (with known abundance) as a proxy for the scattering effects or by performing a physical retrieval of effective parameters for the scattering layer. For GOSAT CH_4 data, these two approaches yield similar precision (~17 ppb) and biases less than 1% compared to TCCON (Wunch et al., 2010), but with lower bias for the proxy method (Schepers et al., 2012). In the proxy retrieval using CO_2, the dry mole fraction of CH_4 (x_{CH4}) is computed by $x_{CH4} = \frac{[CH4]}{[CO2]} x_{CO2}$ where $[CH4]$ and $[CO2]$ are the retrieved columns from spectral radiances that are close in wavenumber and x_{CO2} is the dry mole fraction computed from a global model of atmospheric CO_2 (Frankenberg et al., 2005; Schepers et al., 2012). This method assumes that aerosol scattering modifies the light path for CO_2 and CH_4 spectral absorption in the same way, and that model values for x_{CO2} are accurate.

Retrievals with GFCR measurements are similar to the "proxy retrieval" but they correct the input radiance instead of the retrieved column, and do not make assumptions about aerosol scattering in different spectral bands or rely on knowing CO_2 abundance. CHRONOS uses the D/A signal ratio where D and A are both modified in the same way by aerosol scattering, which has a smooth spectral behavior over the CHRONOS bandpass. This ratio gives an accurate total column amount, but to compute a dry mole fraction (xCH4), we require additional information about the surface pressure (for example, from GOES-16 meteorological data) in order to estimate the dry air column. In general, GFCR retrievals are more resilient than spectral radiance measurements to errors in surface and contaminant species assumptions due to the use of radiance differences and ratios (Pan et al., 1995).

Authors mention single case of aerosol but thin cloud such as high-altitude cirrus is not discussed. Authors proposed use of GOES satellite data for cloud detection but aerosol and thin clouds are difficult to filter out.

As described in Section 4, CHRONOS's primary cloud detection comes through its own GFCR measurements based on many years of experience with MOPITT cloud detection. The fact that CHRONOS is in GEO and making observations of the same scene sub-hourly, also affords some advantages for cloud detection by means of being able to look at very frequent signal differences in combination with GEO imagery from GOES-16 ABI. We have added the following text to Sec. 4:

While the approach of using D/A for retrievals discussed in Section 3.3 will cancel some of the errors due to undetected aerosols or clouds (e.g., thin cirrus), remaining retrievals errors (e.g., O'Dell et al., 2011), particularly for CH_4, will require further study using both CHRONOS radiances and GOES-16 ABI observations.

Specific Comments

(1) Plumes Page 5, Fig 1 Description of diurnal variation of CO emission and typical wind speed in WRF-Chem will help readers' understanding Page 10, Fig. 3 Description of CH4 emission source in Greeley, CO will help readers' understanding.

Clarified: The text of the Figure 1 caption has been updated to state that the WRF-Chem run is driven by analyzed meteorology, and that changes in the distribution of CO are expected as a result of changes in both emissions and meteorology.

Figure 1: Comparison of MOPITT and CHRONOS spatial and temporal coverage over a 5-hour period. The top panels show MOPITT retrievals of near-surface CO for Tuesday Aug. 1, 2006, with pink colors indicating low CO (~ 60 ppbV) and green to red indicating higher values (200 – 300 ppbV). The middle and bottom panels show a simulation of CHRONOS observations using WRF-Chem (Grell et al., 2005) at 4 km horizontal resolution driven by analyzed meteorology (Barth et al., 2012) for the same date. Here blue colors indicate low CO (~60 ppbV), red colors indicate high CO (~300 ppbV) and light greys indicate clouds. Circled areas in the zoomed bottom panels provide detailed examples of changes in CO concentrations over the 5-hour period with pollution from Chicago moving to the west and clouds moving east over the Washington DC area. Urban traffic patterns and weather fronts change the distribution of air pollution throughout the day. Sub-hourly CHRONOS data could assist with attributing the sources of pollution and determining areas affected downwind.

New reference added:

Barth, M. C.**,** Lee, J., Hodzic, A., Pfister, G., Skamarock, W. C., Worden, J., Wong, J., and Noone, D.: Thunderstorms and upper troposphere chemistry during the early stages of the 2006 North American Monsoon, *Atmos. Chem. Phys.*, **12**, 11,003-11,026, doi:10.5194/acp-12-11003-2012, 2012.

Similarly, the text of the Figure 3 caption now includes source description:

Figure 3: Aircraft in situ measurements of CH_4 from the FRAPPE-DISCOVER-AQ in the Colorado Front Range on Aug. 2, 2014. Vertical profiles were measured over cities, identified by spiral flight tracks (each spiral has ~10 km radius). Note that the highest values of CH_4 are plotted last. Total column CH_4 computed from the vertical profiles is different by 4.9% between Ft. Collins (urban) and Greeley (oil/gas and feedlot operations). CHRONOS spatial resolution is indicated by the overlaid grid, illustrating that CHRONOS column measurements would have the spatial resolution and precision to distinguish sub-hourly differences in county-scale CH_4 abundances from space. Data courtesy of Glenn Diskin, NASA.

(2) Page 7, Line 162, It is not clear. Does it mean between 6 and 12%?

Text changed to read "…. between 6 and 12%.".

(3) Page 10, Line 242, "Air quality criteria to protect public health" Reference or explanation is needed.

Clarified: The text referred to has been rewritten as: Nine months before the U.S. Environmental Protection Agency was founded, air quality criteria were established for carbon monoxide (U.S.,

1970) to protect public health in compliance with the 1967 amendments (Public Law 90-148) to the Clean Air Act of 1963 (Public Law 88-206).

(4) Page 12, Line 298 The brief description of the reason why 5μrad is needed.

The text "The displacement between a single paired gas/vacuum measurement is limited to ≤5 μrad/60 msec to ensure acceptable changes in ground pixel reflectance based on MOPITT experience (Deeter et al., 2011), and on simulated radiance errors using representative GEO spacecraft pointing data", has been rewritten to read:

Observation simulation studies using representative GEO spacecraft pointing data have been performed to determine the effect of 'jitter' in spacecraft pointing during the acquisition of a signal pair. The displacement between a single paired gas/vacuum measurement is limited to ≤5 μrad to ensure acceptable changes in ground pixel reflectance based on MOPITT experience (Deeter et al., 2011). This requirement corresponds with a gas cell-to-vacuum cell frame time limited to 60 msec, readily achievable with a physically realistic cell size and rotation frequency, frame acquisition and readout rate. The large (>3000 kg) size of a commercial communications spacecraft therefore serves to naturally attenuate jitter sources over very short time frames, avoiding the need for a costly image stabilization subsystem.

(5) Page 13, Line 313, "the effect of variations in the underling surface" Does it mean fine spectral structure of surface albedo?

Clarified: The text "the effect of variations in the underling surface" has been changed to read "the effects of variations in the underlying surface temperature, emission, and reflectivity".

(6) Page 15, Figure 6, "solid red lines at filter half-power point" Is it 50% transmittance point? The transmittance at red line looks about 40%.

These are the 50% transmittance points, now noted in figure caption.

(7) Page 16, Line 366 (<10%) Accuracy requirement for CO and CH4 must be different but instrument is similar. CO accuracy of 10% is reasonable and was demonstrated with MOPIT. How is the accuracy of 1% achieved in the CH4 retrieval? Aerosol and thin cloud cause bias error and averaging cannot reduce the bias. Recent CH4 satellite retrieval such as GOSAT use O2A band in 0.76 micron to estimate light path modification by aerosol and CH4.

The measurement accuracy requirements of the observations are set by the product accuracy required to answer the science questions (multispectral CO accuracy 10%, and CH_4 accuracy 1% as stated by the Reviewer). Measurement accuracy requirements are discussed in Section 3.2. While the instrument is the same, the measurements of CO and CH4 and the underlying spectral signatures and radiative transfer are different. The CHRONOS instrument acquires fewer or additional observations in each spectral channel to achieve the required signal-to-noise. In Section 3.3, Table1 provides the measurement passbands for optimized spectral sensitivity. We have added to Table 1 the minimum signal-to-noise ratio for each measurement, and the number

of observations needed to achieve that minimum SNR, and supplemented the text preceding the Table as follows:

Table 1 lists the modeled signal-to-noise (SNR) and the total number of individual data acquisitions in each pixel in the 2D detector array ("frames") obtained in a single 9.7-minute data acquisition period, for the minimum radiance case defined from MOPITT on-orbit radiance records. This minimum SNR provides at least 30% margin for meeting the radiance precision requirements.

(8) Page 17, Lines 375-333, "there 3 minute retrieval" "These 3 minute retrieval" and relation between âLij3 min intervals and retrievals are not clear. What is the definition of "single (âLij10 min) data"?

The original text appears to be corrupted. We have rewritten the text to clarify as follows:

Profile or column retrieval precision requirements are achieved in ground processing by averaging geo-located, cloud screened radiances for three minutes (375 separate gas-vacuum measurements for each product: CO [4.6 μm, 800 hPa], CO [4.6 μm, 200 hPa], CO [2.3 μm, 100 hPa]; and 750 measurements of CH_4 [2.2 μm, 800 hPa]). A single retrieval for each product is performed on these averaged radiances. The process of averaging radiances and then retrieving products is repeated for all data acquired in the 9.7-minute data acquisition period.

(9) Page 21, Line 455, "all digital" What do the authors mean by "all digital"? Usually detectors and readout electronics have analogue portion such as amplifier and analogue to digital converter.

The "all-digital" focal plane arrays became available for science use in the early 2000s. For all of the cited arrays, signal amplification and analog-to-digital conversion occur in the readout integrated circuit (ROIC) at each pixel, leading to the term "in-pixel digitization" or "all digital". This type of array is what enables CHRONOS to quantify very small differences in radiance. We have added a reference to:

Brown, M.G., Baker, J., Colonero, C., Costa, J., Gardner, T., Kelly. M., Schultz, K., Tyrrell, B., and Wey, J.: Digital-pixel focal plane array development, Proc. SPIE 7608, Quantum Sensing and Nanophotonic Devices VII, 76082H (January 22, 2010); doi:10.1117/12.838314, 2010.

Although the title above says "digital pixel", text in this and other papers refer to "all digital" or just "digital" focal plane arrays, which is now a common usage we adopt in the manuscript.

(10) Page 22, Line 487, "radiance calibration" Brief description of radiance calibration is needed.

We have added a brief description of radiance calibration to Section 4 as follows:

For on-orbit radiance calibration, CHRONOS views high-precision hot and cold black bodies and deep space for the MWIR channels, and a tungsten lamp (LandSat Operational Land Imager heritage) and a closed aperture for the SWIR calibration within each 10-minute data acquisition.

(11) Page 23, Figure 11, vertical axis "#obs in domain/# pixels Explanation is needed.

Clarified: Added text to the figure caption: "#obs in domain/# pixels (the number of cloud-free pixels observed as a fraction of the total number of pixels in the region)".

(12) Page 30, Line 639, "launch in 2017"

We have changed the GOSAT-2 launch to 2018 at this location and in Table 3.

Page 32 table 3 OCO-3 (2017-) I think GOSAT-2 launch is scheduled to be in 2018 as the authors indicated in Table 3. I think OCO-3 has less possibility to be launched this year.

Table 3 has been revised in response to Reviewer 2.

Technical Corrections

(1) Page 24, Line 522, "total hydrometeors > 10-8/kg/kg" Is it 10^-8?

Corrected: Changed to 10^{-8}/kg/kg.

(2) Page 34, Line 723, "et al." and many others. AMT authors guideline says "Please supply the full author list with last name followed by initials." Other formats also do not meet the guideline.

Corrected: Formats have been changed to match guidelines throughout.

amt-2017-194

The CHRONOS mission: Capability for sub-hourly synoptic observations of carbon monoxide and methane to quantify emissions and transport of air pollution

David P. Edwards, Helen M. Worden, Doreen Neil, Gene Francis, Tim Valle, and Avelino F. Arellano Jr.

Response to Reviewer 2:

We thank the reviewer for their careful evaluation of our manuscript. We address each comment (in blue) with an embedded response (in black) below. We detail new text that has been added to the revised manuscript (in green).

General comments:

The manuscript 'The CHRONOS mission: Capability for sub-hourly synoptic observations of carbon monoxide and methane to quantify emissions and transport of air pollution' by D. P Edwards at al. describes a new mission concept of satellite remote sensing of both trace gases using a geostationary orbit. The proposed instrument is based on MOPITT instrument heritage. Although having such a mission would provide exciting new measurements, the paper itself provides only little scientific news. The MOPITT heritage is discussed extensively in the literature and the possibility to observe CO and CH4 using a geostationary orbit is already discussed e.g. by Butz et al., 2015 and O'Brein et al., 2016.

We respectfully disagree with the comment "the paper itself provides only little scientific news… and the possibility to observe CO and CH4 using a geostationary orbit is already discussed e.g. by Butz et al., 2015 and O'Brein et al., 2016."

The CHRONOS mission concept addresses tropospheric (air pollution) chemistry, specifically, carbon monoxide and methane, the two principal sinks for the hydroxyl radical. Hydroxyl provides the ability of Earth's troposphere to cleanse itself of trace constituents that are harmful and even toxic to plants, animals, and people. When combined with NASA's planned TEMPO observations, CHRONOS observations meet the tropospheric chemistry science objectives of the GEO-CAPE mission (Fishman et al., 2012).

The CHRONOS focus on tropospheric chemistry then results in requirements for frequent time sampling (sub-hourly), and for simultaneous sampling over extended domains ("snapshot") that would be significantly impaired by instrument solutions that take hours to scan a continental domain and sampling patterns that are limited to few times daily, as described in O'Brien et al. (2016) or Butz et al. (2015). An instrument capable of instantaneous observations everywhere over a continental domain with the ability to provide full precision observations everywhere in that domain within 10 minutes is scientific news for meeting the tropospheric chemistry objectives.

Compared to the CHRONOS requirement for CO measurement in two spectral regions, the GeoCARB limitation to CO in one spectral region means that GeoCARB would not able to evaluate vertical pollution transport, or to provide the test of these atmospheric motions as

calculated by advanced atmospheric models (NAS, 2017). The Committee on Earth Observing Satellites (CEOS) has identified the absence of multispectral CO observations after MOPITT as a critical data gap when they met in June 2017.

We agree that MOPITT capabilities are well documented in the literature. An important point of the paper is to report the rationale and specifics of the CHRONOS instrument evolution of MOPITT (CHRONOS provides simultaneous, sub-hourly sampling everywhere in the domain instead of temporally discontinuous orbital tracks with, at best, daily revisit; and CHRONOS improves spatial resolution to 4 km x 4 km from MOPITT's 22 km x 22 km).

the downstream from mission objectives to instrument and product requirements is not always traceable for me… Sec 2.2 …. already concludes that CHRONOS meets all the objectives although the instrument …. is discussed much later in the paper

This paper was written with the intent of laying out the science case first and then describing the measurement requirements and instrument. This may be different to some instrument papers, but it is also becoming a frequent style for papers, reports, and surveys following the "Traceability Matrix" approach (e.g., NRC, 2007, and the currently in-process NASA/NOAA/USGS 2017 Decadal Survey).

science objectives for CH4 geo observations are not always convincing to me

Section 6.2 discusses OSSEs by Wecht et al. (2014) that evaluated the potential of hourly methane observations (such as we describe in this paper) for constraining emissions. Wecht et al. report that hourly observations constrain methane emissions more than a factor of two better than daily observations (TROPOMI), and significantly better than GOSAT.

it is not clear to me if air quality forecast can really be improved with these uncertainties

At the end of Section 2.2, we describe previously published OSSE studies that show the benefit, compared to the ground-based monitoring network, of high spatial and temporal resolution sampling from GEO in constraining transport patterns and in constraining the distribution of near-surface CO concentrations. Specifically, Edwards et al (2009) cites improved skill scores for near surface CO, and Zoogman et al (2014) demonstrates improvements to near surface ozone from joint CO-ozone assimilations.

Specific comments:

1. Figure 1: What is the spatial coverage of the MOPITT panels? For a better comparison, both MOPITT and WRF-Chem images should use the same color code, which should be indicated in a corresponding figure legend.

Details of the MOPITT instrument are included in the references in the Introduction. MOPITT uses a cross-track scan of 640 km that allows for almost complete coverage of the Earth's surface in about 3 days, with pixels of 22 km x 22 km horizontal resolution. The intent of Figure 1 is to

graphically depict spatial coverage as a function of hourly sampling for MOPITT compared to what might be seen from CHRONOS. It is not intended as a comparison of MOPITT CO values with the WRF-Chem model. Validation of MOPITT against both models and observations, taking into account averaging kernel sensitivity and a priori assumptions not considered in this figure, are covered by the MOPITT references in the manuscript (and references therein).

2. Figure 3: The figure shows CH4 in situ measurements with significant enhancements whereas changes in the total column is much less (4.9 %). I think this enhancement is given on the spatial sampling of the in situ measurements but do not necessarily represent the CH4 enhancement for a 4x4 km2 sampling of CHRONOS. I can imagine this makes a different.

While the individual in-situ measurements shown in Fig. 3 are indeed not at the CHRONOS spatial resolution, the methane enhancements observed near oil/gas and feedlot operations during the 2014 FRAPPE DISCOVER-AQ campaign were persistent over the spiral flight tracks shown, each spiral with an approximate radius of 10 km (see e.g, Flynn et al., 2016). The total column calculation that yields the quoted 4.9 % difference therefore corresponds to the CHRONOS pixel scale. As the reviewer points out, high methane values at very small scale, as might be expected from an individual pipe leak, would not probably not produce the necessary column enhancement to be detected at the CHRONOS pixel scale. We are careful to suggest emissions estimates for CH_4 at the county-level spatial scales (~40 km x 40 km) as demonstrated in the referenced OSSE by Wecht et al. (2014a) as part of the studies for GEO-CAPE.

We clarify this in the revised Figure 3 caption: Vertical profiles were measured over cities, identified by spiral flight tracks (each spiral has ~10 km radius).

3. Figure 4 and 12: These figures do not present new material and can be discussed in the text with appropriate references.

While this material may be understood by some readers, these figures have never before been published and we think they help elucidate the CHRONOS measurement concepts much more clearly than we could describe with text. We have found frequently that audiences are not familiar with the principles of GFCR, as compared to more usual grating spectrometer or FTIR measurement approaches. CHRONOS also employs alternating gas/vacuum cells, which is different to the MOPITT pressure-modulated and length-modulated GFCR technique. For these reasons, we believe that Figure 4 provides valuable context.

Clarified: Specified 'the CHRONOS GFCR measurement' in the text of the Figure 4 caption.

A similar comment applies to Figure 12. Of all the current and planned CO measuring instruments, MOPITT is the only one making multispectral CO retrievals. The other instruments either make SWIR column measurements or TIR mid-troposphere measurements. As a result, readers who are not familiar with the MOPITT literature will not appreciate the advantage of the multispectral approach in providing independent near-surface CO concentrations to understand emissions and pollution transport. This is a primary motivation for the CHRONOS concept.

4. Page 23, line 509: To my knowledge, it is not demonstrated that CH4 can be retrieved from real MOPITT data with a cloud coverage of 5 %. I doubt that this is possible considering the strict

cloud filtering of GOSAT observations for CH4 retrieval.

As outlined in Section 3.3 and references therein, MOPITT does not retrieve CH4 with or without clouds, due to well-documented instrumental issues.

It is an advantage of GFCR that 'contaminating' signals that are spectrally flat across the radiometer filter passband are effectively cancelled out by the D/A signal. We have added a description to Section 4 as follows:

While the approach of using D/A for retrievals discussed in Section 3 will cancel some of the errors due to undetected aerosols or clouds (e.g., thin cirrus), remaining retrievals errors (e.g., O'Dell et al., 2011), particularly for CH_4, will require further study using both CHRONOS radiances and GOES-16 ABI observations.

5. Page 19 line 414: The aerosol optical depth should be provided at a reference wave- length within the SWIR fit window. Depending on the size of the aerosol parameter, this can be very small.

The value of AOD used in the 2.25 micron SWIR window aerosol simulation was 0.089. This is now added to the text. This aerosol case was chosen to represent high pollution loading with the most significant AOD values in our SWIR window.

We have added to Figure 7 caption: (...AOD is 0.089, which is obtained by scaling the OPAC urban aerosol case by 1.5)

6. Table 2: I think, a discussion for elevated aerosol layers and cirrus is needed for a better error estimate. From other missions, we know that these are relevant error sources.

We agree that this is a tricky problem and we expect to use the CHRONOS radiances as well as GOES-16 ABI cloud measurements to diagnose and potentially flag observations that might not be properly filtered by our cloud detection approach. We will also follow the approaches identified for OCO-2 observations to detect and quantify retrieval errors due to undetected aerosol and thin cirrus clouds (e.g., O'Dell et al., 2011). We have added discussions to Section 3.2 in response to Reviewer 1 and to the cloud detection paragraph in Section 4 as noted in Specific comment 4 above.

7. Table 2: Here a precision requirement of <10 % is given, whereas Fig 2 indicates that urban air quality daily evolution is in the order of 1-2 ppm. I doubt that with this large precision, urban daily evolution can be measured. See also page 17, line 383-385.

We recognize the opportunity for confusion between ppm and ppb and have corrected Figure 2 to show 1000-2000 ppb rather than 1-2 ppm for CO. Precision requirement of 10% is approximately 10 ppb based on global average abundance of CO.

8. Page 15 line 335-340. The SCIAMACHY CH4 product is inferred from 1.6 micron measurements, GOSAT also uses the methane sensitivity at 1.6 micron, which in both cases differ from the CHRONOS SWIR window at 2.2 micron.

The measurement of CH4 at 2.2 microns was considered by SCIAMACHY prior to the detector icing problem, is used by S5-P/TROPOMI, and will be used by GeoCARB. The spectral band used for methane is summarized in the new Table 3.

9. Section 6: I am not sure if I overlooked it, but when discussing synergies with other mission an indication of a launch window is required. I think, also the Sentinel-5 mission and IASI-NG should be mentioned here.

We have revised Table 3 to reflect a CHRONOS launch no earlier than (NET) 2024 and have included Sentinel-5. We chose not to include IASI-NG as it makes observations only in the MWIR (similar to other sounders such as the current IASI instrument and CrIS). As described in Sections 5.1 and 6.1, these instruments do not generally have measurement sensitivity to the full column.

I also miss a discussion of GEOCarb, which would measure CO, CO2 and CH4. Because the mission concept is already published, it should not be ignored in this manuscript.

We have added a discussion of GeoCARB in Section 6 and in the revised Table 3.

10. Table 3: This table does not provide new information, which is not already discussed in the text. It also does not fit the format of a science publication to my opinion.

We have revised Table 3 to include only details of CO and CH_4 measurements.

The CHRONOS mission: Capability for sub-hourly synoptic observations of carbon monoxide and methane to quantify emissions and transport of air pollution

David P. Edwards[1], Helen M. Worden[1], Doreen Neil[2], Gene Francis[1], Tim Valle[3], and Avelino F. Arellano, Jr.[4]

[1]National Center for Atmospheric Research (NCAR), Boulder, CO, USA
[2]NASA Langley Research Center, Hampton, VA, USA
[3]Ball Aerospace, Boulder, CO, USA
[4]University of Arizona, Tucson, AZ, USA

Correspondence to: D. P. Edwards (edwards@ucar.edu)

Abstract. The CHRONOS space mission concept provides time-resolved abundance for emissions and transport studies of the highly variable and highly uncertain air pollutants carbon monoxide and methane, with sub-hourly revisit rate at fine (~ 4 km) horizontal spatial resolution across a North American domain. CHRONOS can provide complete synoptic air pollution maps ("snapshots") of the continental domain with fewer than 10 minutes of observations. This rapid mapping enables visualization of air pollution transport simultaneously across the entire continent and enables a sentinel-like capability for monitoring evolving, or unanticipated, air pollution sources in multiple locations at the same time with high temporal resolution. CHRONOS uses a compact imaging gas filter correlation radiometer for these observations, with heritage from more than 17 years of scientific data and algorithm advances by the science teams for the MOPITT instrument on NASA's Terra spacecraft in low Earth orbit. To achieve continental-scale sub-hourly sampling, the CHRONOS mission would be conducted from geostationary orbit, with the instrument hosted on a communications or meteorological platform. CHRONOS observations would contribute to an integrated observing system for atmospheric composition using surface, suborbital and satellite data with atmospheric chemistry models, as defined by the Committee on Earth Observing Satellites. Addressing the U.S. National Academy's 2007 Decadal Survey direction to characterize diurnal changes in tropospheric composition, CHRONOS observations would find direct societal applications for air quality management and forecasting to protect public health.

1 Introduction

For the end of the current decade, geostationary Earth orbit (GEO) satellite missions for atmospheric composition are planned over North America, East Asia and Europe, with additional missions in formulation or proposed. Together, these present the possibility of a constellation of GEO platforms to achieve continuous, time-resolved, high-density, observations of continental domains for mapping pollutant sources and variability on diurnal and local scales with near-hemispheric coverage (CEOS, 2011). In addition to NASA's TEMPO mission (Zoogman, 2017), the ESA/EUMETSAT Sentinel 4 mission over Europe (GMES-GAS, 2009) and the Korean KARI MP-GEOSAT/GEMS mission over Asia (Lee et al., 2010), will provide data products for ozone (O_3), nitrogen dioxide (NO_2), sulfur dioxide (SO_2), formaldehyde (HCHO) and aerosol optical depth (AOD) several times per day with smaller than 10 km x 10 km spatial footprints. While these planned GEO measurements will provide new information on the diurnal evolution of emissions and chemical transformation of some important pollutants, they are missing observations of methane (CH_4) and carbon monoxide (CO). As identified in CEOS (2011), these gases play key roles in atmospheric chemistry, air quality and climate.

The planned GEO constellation will be further enhanced by current and upcoming low Earth orbit (LEO) missions with atmospheric composition measurement capability. These missions include OMI (Ozone Monitoring Instrument, Levelt et al., 2006), IASI (Infrared Atmospheric Sounding Interferometer, Clerbaux et al., 2009), CrIS (Cross-track Infrared Sounder, Gambacorta et al., 2014), OMPS (Ozone Mapping Profiler Suite, Flynn et al., 2014), and the ESA Sentinel-5 precursor mission, TROPOMI (Veefkind et al., 2012). The LEO assets allow for a transfer-standard between the GEO missions, filling gaps in the spatial coverage, enabling cross-calibration and validation, and potentially, combined data products. Such an integrated global observing system for atmospheric composition is key to abatement strategies for air quality as prescribed in international protocols and conventions (e.g., IGACO, 2004).

Pollution affecting air quality is a complex mixture of many compounds that was designated a Group 1 carcinogen by the World Health Organization (WHO) (Loomis et al., 2013) amidst rising concerns about increased mortality and economic costs. Outdoor air pollution causes pulmonary and cardiovascular diseases, lung cancer, and premature birth (Brunekreef and Holgate, 2002; Turner et al., 2015; Fann et al., 2012, Malley et al., 2017). Despite improvements in U.S. air quality

in recent decades, present-day levels of air pollution decrease average life expectancy by 0.7 years and contribute to 10% of the total deaths in highly polluted areas such as Los Angeles (Fann et al., 2012). In 2010, over 3% of U.S. preterm births were attributed to air pollution at an estimated cost exceeding $5 billion (Trasande et al., 2016). To address the causes of air pollution effectively, decision makers need comprehensive measurements to quantify the full suite of pollutants, including CH_4 and CO, emitted from industrial, transport and energy sectors, as well as natural sources. CO, which allows detection of combustion-related emissions, serves as the reference for the emissions of many difficult-to-measure pollutants that impact air quality and climate. Wildfires, which emit both CO and CH_4, are a particular concern in the Western U.S. (Abatzoglou and Williams, 2016), where burn areas have increased by a factor of 6 since 1970, with severe economic impacts (Westerling et al., 2006). CO and CH_4 emissions also have significant consequences for climate change, especially considering CH_4 pollution due to recent large increases in natural gas production (Pétron et al., 2012; Miller et al., 2013) and potential new CH_4 releases from thawing permafrost (Ciais, 2013).

After air pollutants are emitted, they are transported vertically and horizontally in the atmosphere and can have a significant impact on local air quality and human health at locations near the sources and also downwind. Distinguishing the relative contributions of local and non-local pollution sources has emerged as a fundamental challenge for air quality management in the U.S. (NRC, 2004). Because CO has a medium lifetime (weeks to months), it can be transported globally, but does not become evenly mixed in the troposphere. This moderate lifetime makes CO an ideal tracer of combustion-related air pollution (e.g., Edwards et al., 2004; 2006).

The CHRONOS mission is motivated by these fundamental questions regarding the emissions and transport of air pollutants. The CHRONOS gas filter correlation radiometry (GFCR) measurement technique for multi-spectral CO builds on 17 years of observations from the NASA Terra satellite Measurements of Pollution in the Troposphere (MOPITT) instrument (Drummond et al., 2010, H. M. Worden et al., 2013), in addition to experience in LEO column CH_4 retrievals from SCIAMACHY (Frankenberg et al., 2005; 2011) and GOSAT (Morino et al., 2011; Schepers et al., 2012). The CHRONOS temporal resolution (sub-hourly), and spatial resolution (nominally 4 km × 4 km at the domain center), are required to capture the near surface trace gas variability, as concluded by modeling and data studies performed by the Geostationary Coastal & Air Pollution Events (GEO-CAPE) (Fishman et al., 2012) science team in response to the first Decadal Survey

for Earth Science and Applications (NRC, 2007). For CH_4, the spatially and temporally dense CHRONOS measurements over the entire continental U.S. measurement domain would address the need for consistent assessments of CH_4 emissions at decision-relevant scales. For CO, proven multispectral retrieval techniques (Worden et al., 2010) increase the information on CO vertical distribution, and can identify vertical transport from one observation to the next. Thus, CHRONOS is capable of tracking pollutants from the surface where they are emitted, to where they degrade downwind air quality.

This paper describes the CHRONOS science, measurement technique, expected performance (precision and accuracy), retrieval vertical sensitivity and observing strategy. We then show how CHRONOS would complement observations from other current and planned satellite instruments, and conclude with a summary of CHRONOS features and advantages.

2 CHRONOS Science

2.1 CHRONOS Sub-hourly Synoptic Measurements with High Spatial Resolution

Advances in tropospheric remote sensing from LEO over the past decade have shown the potential of satellites to quantify the sources, transport and distributions of the gases important for air quality and climate (NRC, 2007; Simmons et al., 2016). LEO data provide valuable knowledge on continental to global-scale pollution, but their spatial and temporal resolution, sparseness of coverage, and often large uncertainties for individual trace gas observations, have so far limited their use in understanding air pollution sources and distributions on local to regional spatial scales (Figures 1 and 2).

The importance of sub-hourly time resolution for capturing the diurnal evolution of pollution transport is shown in Figure 1, which compares current MOPITT measurement sampling to that which would be obtained from CHRONOS over the continental U.S.

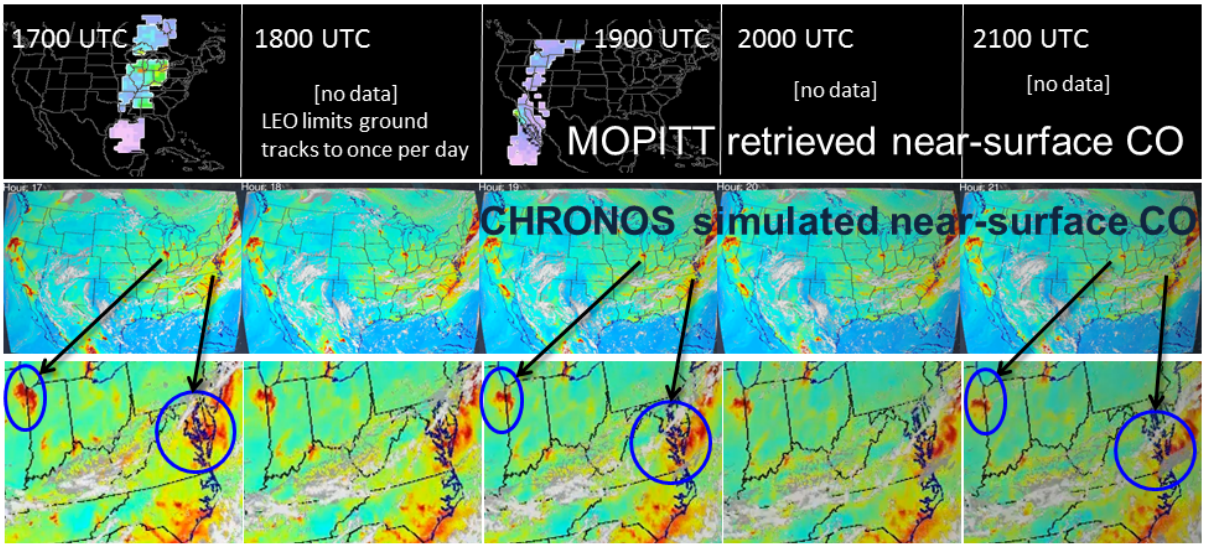

Figure 1: Comparison of MOPITT and CHRONOS spatial and temporal coverage over a 5-hour period. The top panels show MOPITT retrievals of near-surface CO for Tuesday Aug. 1, 2006, with pink colors indicating low CO (~ 60 ppbV) and green to red indicating higher values (200 – 300 ppbV). The middle and bottom panels show a simulation of CHRONOS observations using WRF-Chem (Grell et al., 2005) at 4 km horizontal resolution driven by analyzed meteorology (Barth et al., 2012) for the same date. Here blue colors indicate low CO (~60 ppbV), red colors indicate high CO (~300 ppbV) and light greys indicate clouds. Circled areas in the zoomed bottom panels provide detailed examples of changes in CO concentrations over the 5-hour period with pollution from Chicago moving to the west and clouds moving east over the Washington DC area. Urban traffic patterns and weather fronts change the distribution of air pollution throughout the day. Sub-hourly CHRONOS data could assist with attributing the sources of pollution and determining areas affected downwind.

Understanding the rapidly changing tropospheric state and critical processes that are episodic or have diurnal timescales, such as traffic emissions, forest fire intensity, meteorology and changes in the planetary boundary layer (PBL) height, requires temporal resolution that is better than once a day (Fishman et al., 2012). Accurate prediction of air quality requires an observing framework for atmospheric composition similar to that for weather forecasting, where instruments in GEO are essential components of the integrated observing system and complement existing LEO, suborbital, and surface assets and modeling capability. As such, CHRONOS in GEO addresses the

need for sub-hourly vertical and horizontal transport information for "chemical weather" prediction.

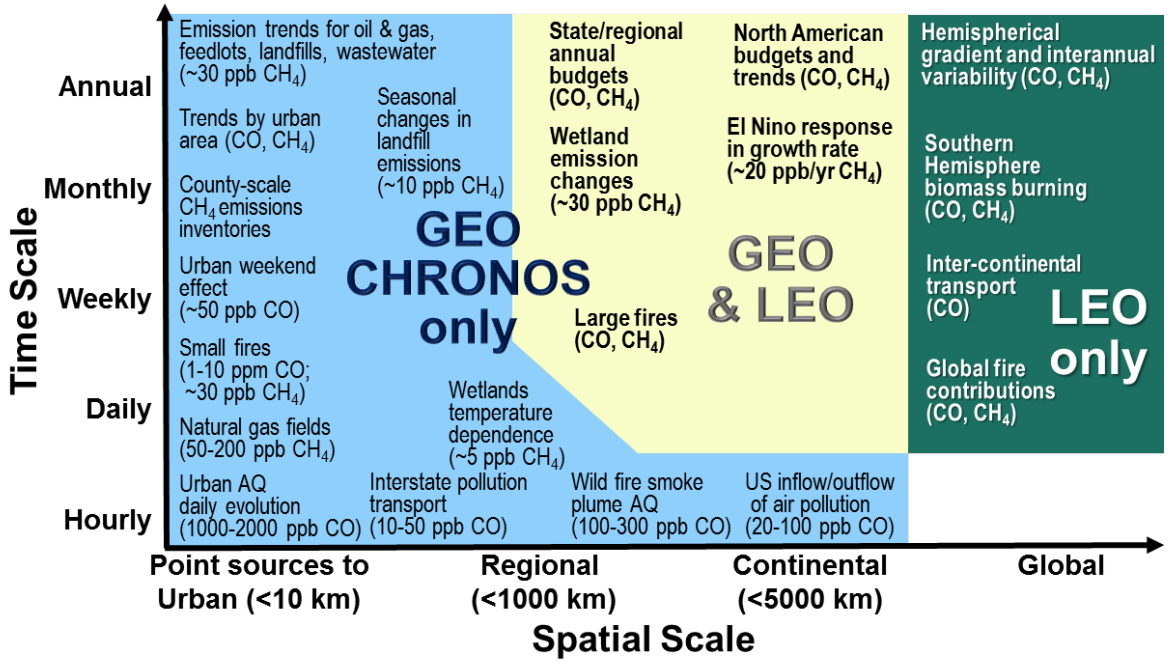

Figure 2: CHRONOS' sub-hourly observations would provide access to the fine temporal and fine spatial scales of CH_4 and CO processes for understanding the emissions and transport of air pollution for air quality, climate, and energy management applications. Estimated abundances are for process contributions above background levels.

2.2 The CHRONOS Science Objectives

CHRONOS focuses on two interrelated science objectives: emissions of highly variable and poorly quantified air pollutants, and air pollution transport across North America. Significant scientific advances in understanding these air pollutant emissions and transport processes are expected to lead to improvements in chemical transport model predictability on both regional and global scales.

Objective 1 – Emissions: *Quantify the temporal and spatial variations of CH_4 and CO emissions for air quality, climate, and energy decision making.*

Large uncertainties and conflicting estimates exist in current CO and CH_4 emissions. Aircraft data show National Emissions Inventory (NEI) CO emissions are too high by a factor of 3 in the summer (Hudman et al., 2008; Miller et al., 2008). Satellite data, including MOPITT, indicate

large seasonal changes in CO emissions with a maximum in winter and minimum in summer (Kopacz et al., 2010), that are currently absent from the NEI, and show fire emissions that are too low by as much as 30% (Pechony et al., 2013). Measurements of CH_4 from surface and aircraft observations imply that the EPA 2009 emission inventory is too low, by about a factor of 2, due to large uncertainties from fossil fuel production (coal and natural gas fields, especially in the Western States and Canadian tar sands), transportation, agriculture, wetlands, and thawing permafrost in Canada (Katzenstein et al., 2003; Xiao et al., 2008; Kort et al., 2008; Pétron et al., 2012; Miller et al., 2013; Pechony et al., 2013; Schwietzke et al., 2016). In particular, for natural gas production, recent studies present conflicting results. Karion et al. (2013) showed between 6 and 12% CH_4 leakage from gas and oil production fields in Unitah County, Utah, using airborne measurements, while Allen et al. (2013) found less than 1% leakage at 190 U.S. natural gas sites using emissions activity estimates. Recent research identified sensor issues in the surface measurements used by natural gas companies often causing under-estimated emissions (Howard et al., 2015). These observational inconsistencies can be resolved by comprehensive measurements that are temporally and spatially dense.

CO observations also serve as proxy for other pollutant emissions. Emissions of other combustion pollutants that are important to air quality and climate are frequently correlated with CO emissions, including other ozone and aerosol precursors (Edwards et al., 2004; Massie et al., 2006; Zhang et al., 2008; Bian et al., 2010). As a result, the emission inputs to chemical transport models for many combustion-related species are specified by ratios referenced to CO. CO serves as a proxy for anthropogenic carbon dioxide (CO_2) (Palmer et al., 2006; Worden et al., 2012; Silva et al., 2013) and black carbon (BC) sources (Arellano et al., 2010). CH_4 correlations with CO distinguish CH_4 from fires (J. Worden et al., 2013). Assimilation of CHRONOS data into regional scale chemical transport models would leverage inter-species constraints to allow the emissions and distributions of correlated species to be inferred using CHRONOS measurements (e.g., Gaubert et al., 2016).

Objective 2 – Transport: *Track rapidly changing vertical and horizontal atmospheric pollution transport to determine near-surface air quality at urban to continental spatial scales, and at diurnal to monthly temporal scales.*

Source attribution for local and transported pollution is an important step toward attaining air quality standards (NRC, 2004). Understanding the production of air pollution requires knowledge

of ozone and aerosol precursor emissions (CO and CH_4 among them), and the transport of both precursors and other air quality pollutants (for example, using CO as a tracer). Air pollution crosses international and state boundaries to impact downwind cities, national parks, and wilderness areas. The Cross-State Air Pollution Rule (U.S. EPA, 2011) requires 23 states to reduce emissions in order to meet air quality standards in downwind states. Considerable international efforts are directed toward understanding intercontinental transport of air pollution (Galmarini et al., 2017). CHRONOS' multispectral retrievals of CO would provide the vertical sensitivity to determine transport out of the PBL, into the free troposphere, and the vertical descent back to the surface at some distance downwind. This new CHRONOS information would allow state and local air quality managers to quantify interstate pollution, along with intermittent sources such as fires that affect the ability of urban areas to meet air quality standards.

The time and space scales of CHRONOS measurements are designed to be similar to the scales of models for regional air quality applications, leading to improvements in process representation. From observing system simulation experiments (OSSEs), we have demonstrated that data assimilation of simulated CHRONOS multispectral observations of CO significantly improves comparisons with the "true" surface CO values at EPA surface monitoring sites (Edwards et al., 2009). Sub-hourly measurements of CO throughout the troposphere would allow for more frequent data assimilation updates than is currently possible, which, along with increased accuracy in surface CO knowledge, would dramatically improve the skill for air quality prediction. OSSEs also demonstrate that CHRONOS' CO measurements augment TEMPO's ozone measurement capability through joint ozone-CO data assimilation (Zoogman et al., 2014).

2.3 CHRONOS Measurements of CH_4 and CO

More than half of CH_4 emissions are anthropogenic, with contributions from fossil-fuel production, animal husbandry and waste management, while wetlands are the primary natural source (Bergamaschi et al., 2009). CH_4 has an atmospheric lifetime of 8–10 years, and exerts 86 times the global warming potential of CO_2 emissions on a 20-year timeframe (Myhre et al., 2013). The U.S. is presently the world's largest producer of natural gas (Breul et al., 2013). Production has increased 20% since 2008, with a corresponding need to quantify how much CH_4 is released during extraction. Furthermore, CH_4 has an impact on air quality as a precursor to tropospheric ozone and aerosols through changes in hydroxyl radical (OH) (Shindell et al., 2009). CH_4 thus

plays a pivotal role in both air quality and climate, and co-benefits to both air quality and climate may arise from reducing CH_4 emissions (West et al., 2006; Shindell et al., 2009; UNEP, 2011; Schneising et al., 2014). CHRONOS' frequent (sub-hourly) CH_4 observations would provide the information needed to resolve discrepancies in CH_4 emissions at the county, decision-making, scale.

Dense data sampling improves the capability for constraining model emissions (e.g., Bousserez et al., 2016; Wecht et al., 2014 a). Figure 3 shows a grid representing the CHRONOS spatial resolution overlaid on aircraft measurements taken during the FRAPPE-DISCOVER-AQ field campaign (Pfister et al., 2017) in the Colorado Front Range on Aug. 2, 2014. This indicates high CH_4 in areas of extensive oil and gas extraction and feedlot operations in Colorado (Greeley and Platteville), as compared to other urban and rural locations. By comparison, CH_4 concentrations during the 2015 Aliso Canyon leak (Conley et al., 2016), over the Los Angeles basin were an order of magnitude higher than these Colorado oil and gas concentrations, and thus could have been quantified from space using CHRONOS CH_4 observations, had they been available. Recent studies have demonstrated the potential for using CO and CH_4 satellite data to constrain sources using adjoint and other inversion models (Bergamaschi et al., 2007; 2009; Meirink et al., 2008; Kopacz et al., 2009; 2010; Fortems-Cheiney et al., 2011; Pechony et al., 2013; Wecht et al., 2014b; Turner et al., 2015; Jacob et al., 2016). These studies also show that present ability to optimize emission estimates is limited by the sparse sampling of present measurements. CHRONOS would provide the data density and near-surface abundance information that are needed in adjoint inversions for CO and CH_4 emissions estimates with the spatial and temporal resolution necessary to understand emission inventory errors.

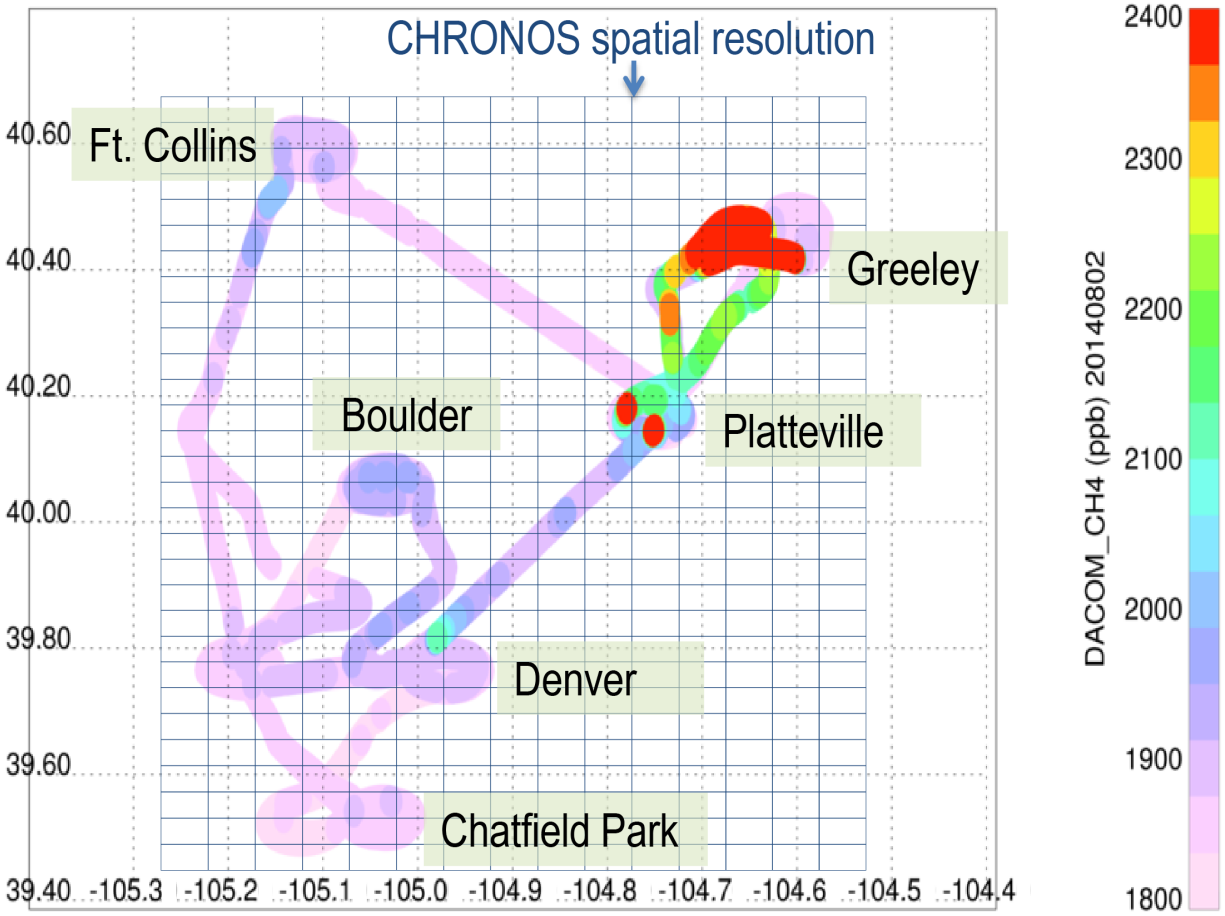

Figure 3: Aircraft in situ measurements of CH_4 from the FRAPPE-DISCOVER-AQ in the Colorado Front Range on Aug. 2, 2014. Vertical profiles were measured over cities, identified by spiral flight tracks (each spiral has ~10 km radius). Note that the highest values of CH_4 are plotted last. Total column CH_4 computed from the vertical profiles is different by 4.9% between Ft. Collins (urban) and Greeley (oil/gas and feedlot operations). CHRONOS spatial resolution is indicated by the overlaid grid, illustrating that CHRONOS column measurements would have the spatial resolution and precision to distinguish sub-hourly differences in county-scale CH_4 abundances from space. Data courtesy of Glenn Diskin, NASA.

Nine months before the U.S. Environmental Protection Agency was founded, air quality criteria were established for CO (U.S., 1970) to protect public health in compliance with the 1967 amendments (Public Law 90-148) to the Clean Air Act of 1963 (Public Law 88-206). CO is produced by combustion processes, including transportation, manufacturing, agricultural burning,

and wildfires, and by hydrocarbon oxidation. CO participates in the formation of ground level ozone; and, as the dominant sink for the main tropospheric oxidant, OH, CO plays a central role in determining the ability of the atmosphere to cleanse itself of pollutants (e.g., Holloway et al., 2000) and thus affects the lifetime of CH_4 (Myhre et al., 2013). The CO lifetime of ~2 months provides time for CO to be transported globally, yet is sufficiently short to show large contrasts between polluted air and the background atmosphere (Edwards et al., 2004). For these reasons, CO is one of the few mission-critical measurements in all aircraft campaigns of the NASA Global Tropospheric Chemistry Program (Fisher et al., 2010) and similar regional air pollution studies. CHRONOS would use the CO multispectral retrieval created by the MOPITT team providing enhanced sensitivity to near-surface CO concentrations (Worden et al., 2010; Deeter et al., 2013). This allows CO plumes near the surface to be distinguished from plumes in the free troposphere to quantify how sources of CO impact downwind regions (Huang et al., 2013). This approach is discussed in Section 5.

3 The Gas Correlation Filter Radiometry (GCFR) Measurement technique

3.1 GCFR Concepts

Gas filter correlation radiometry features extremely high spectral selectivity combined with high throughput to enable precise measurements of atmospheric trace constituents such as CH_4 and CO. GCFR (Acton et al., 1973, Ludwig et al., 1973, Tolton and Drummond, 1997) has been used for satellite remote sensing on Space Shuttle/MAPS (Reichle et al., 1999), UARS/ISAMS and HALOE (Rodgers et al., 1996; Russell et al., 1993), and Terra/MOPITT (Edwards et al., 1999; Drummond et al., 2010). The pioneering MAPS instrument used two detectors with careful electronic balancing on its four Space Shuttle flights to measure CO, and MOPITT uses length and pressure modulation of a single cell, rather than separate gas and vacuum cells, for its successful observations during more than 17 years in LEO. Correlation radiometers have thus proven rugged and reliable in space. The first Decadal Survey for Earth Science and Applications recommended "an IR correlation radiometer for CO mapping" and also stated that the "Combination of the near-IR and thermal-IR data will describe vertical CO, an excellent tracer of long-range transport of pollution (NRC, 2007)."

The GFCR technique is based on the concept that the near ideal filter for the spectral signal from a particular molecule comes from the molecule itself. The effective spectral resolution of the GFCR response function (Edwards et al., 1999, figure 3) matches the pressure-broadened Lorentz full-width-half-maximum (FWHM) for weak-absorption lines (Beer, 1992), and ranges from 0.08 cm^{-1} to 0.16 cm^{-1} for 200 hPa to 800 hPa GFCR gas cells (Pan et al., 1995). This optimal spectral resolution for measuring tropospheric trace gas absorption and for probing the spectral line profile to obtain information on the trace gas atmospheric vertical distribution is difficult to achieve for most spectrometers without sacrificing signal amplitude (grating spectrometers) or increasing noise (Fourier transform spectrometers). The limitation for the GFCR technique is that atmospheric retrievals are made only for those gases contained within the cells of the instrument. However, for observations of CO and CH_4 from GEO (50 times farther from Earth than LEO), the advantages of both high effective spectral resolution and high throughput provided by CHRONOS's gas filter correlation radiometry make for a particularly robust measurement approach.

In the GFCR technique, shown schematically in Figure 4, the top-of-atmosphere (TOA) spectral radiance from each observed field of view (FOV) passes through an instrument cell containing the same gas as the atmospheric target gas being measured, either CO or CH_4 in the case of CHRONOS. The instrument cell uses the gas of interest as a highly selective filter to match narrow spectral features in the atmosphere. With known gas cell dimensions, gas content, temperature and pressure, this technique provides nearly perfect spectral knowledge. The GFCR method efficiently filters the target gas information from surrounding spectral interference, while simultaneously measuring and integrating the target spectra across the selected spectral bandpass, delivering a spectral response function that can be accurately calibrated because it is defined by the cell gas absorption. For these reasons, thorough GFCR instrument characterization is needed prior to launch, along with on-orbit radiometric calibration and measurements of cell parameters (Neil et al., 2010).

Idealized implementation of gas filter correlation radiometry requires viewing the same scene through the same optics with the same detector for each of two gas cells (one containing the gas of interest and the other containing a vacuum (or a gas with no spectral signature in the selected spectral region). The goal is that the ratio of the spectral radiance viewed through the two cells is only a function of the target gas. Spatial misalignment of the two measurements could result in

changes in the viewed surface reflectivity, and thus radiance changes in gas-vacuum cell difference. Temporal offsets could result in different atmospheric paths being captured because of target gas or cloud movement through the field of view. Changes in the instrument function between gas and vacuum views (different optics or detector) are equivalent to radiance errors. The CHRONOS implementation provides nearly simultaneous acquisition of the gas and vacuum cell signals through a common optical path, and minimizes ground co-registration errors between signal pairs. Observation simulation studies using representative GEO spacecraft pointing data have been performed to determine the effect of 'jitter' in spacecraft pointing during the acquisition of a signal pair. The displacement between a single paired gas/vacuum measurement is limited to ≤5 μrad to ensure acceptable changes in ground pixel reflectance based on MOPITT experience (Deeter et al., 2011). This requirement corresponds with a gas cell-to-vacuum cell frame time limited to 60 msec, readily achievable with a physically realistic cell size and rotation frequency, frame acquisition and readout rate. The large (>3000 kg) size of a commercial communications spacecraft therefore serves to naturally attenuate jitter sources over very short time frames, avoiding the need for a costly image stabilization subsystem.

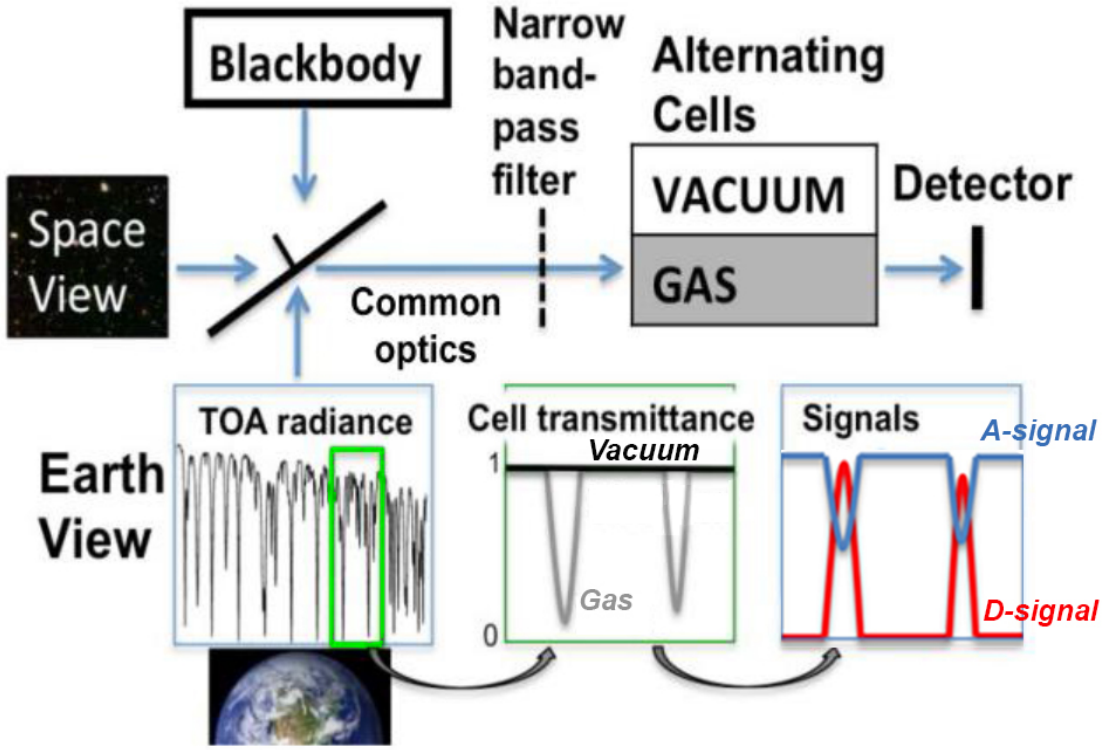

Figure 4: Simplified depiction of the CHRONOS GFCR measurements to show how Average (A) and Difference (D) signals are generated from measurements through the vacuum (V) and gas (G)

cells. Upwelling atmospheric radiance passes through a narrow bandpass filter, selected for the target gas spectral range, a target gas cell, and on to a detector pixel. For CHRONOS, within 60 msec, the atmospheric radiance passes through an identical bandpass filter, an identical reference vacuum cell, and falls on the same detector pixel.

In gas filter correlation radiometry, the relationship of the instrument analog signal and the actual spectrum must be interpreted using a forward atmospheric model and line-by-line spectral radiative transfer calculations (Pan et al., 1995). For instrument development, these calculations form the basis of the instrument spectral characteristics definition (bandpass and width for each target gas and spectral region), and quantify the instrument sensitivity to the target gas, the effects of signatures of non-target gases in the selected spectral region, and the effects of variations in the underlying surface temperature, emission, and reflectivity. After launch, these calculations are a crucial part of the instrument model used in data retrieval.

3.2 Spectroscopy of CO and CH_4 and the CHRONOS Instrument Signals

Two CO spectral bands, the mid-wave infrared (MWIR) fundamental at 4.6 μm (Figure 5) and the short-wave infrared (SWIR) overtone band at 2.3 μm (Figure 6), are the only spectral regions that produce CO features easily distinguished from the surrounding spectra at wavelengths shorter than microwave, and thus are useful for passive remote sensing of tropospheric CO (e.g., Edwards et al., 1999; 2009). Measurements in the MWIR band rely on thermal emission from the Earth's surface and atmosphere (that can be obtained both day and night), and relatively strong spectral features. Measurements in the MWIR are only sensitive to changes in lower atmosphere CO concentration when sufficient thermal contrast exists between the surface and near-surface atmosphere (Deeter et al., 2004). Typically, MWIR signals are most sensitive to CO concentration changes in the mid-troposphere, where long-range pollution transport typically occurs. In contrast, measurements in the CO SWIR band rely on solar radiation reflected from the Earth's surface in daylight, with comparatively weak CO spectral features (Deeter et al., 2009). Typically, the SWIR signal has almost uniform sensitivity to changes in the CO vertical profile, including information near the surface.

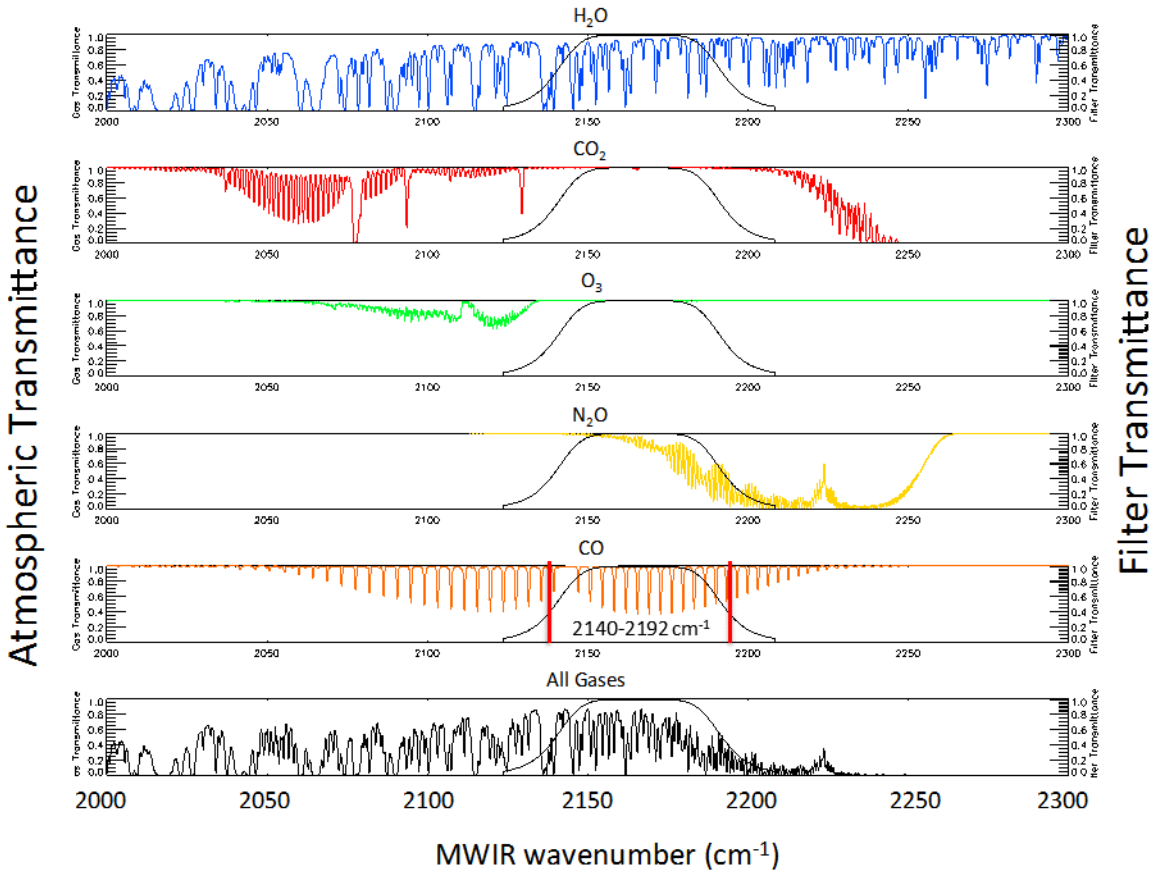

Figure 5: Atmospheric transmittance for primary trace gases in the MWIR vs. wavenumber. The CHRONOS filter transmission is indicated by smooth bandpass curves with solid red lines at filter half-power points (50% transmittance). CHRONOS measures only CO in the MWIR.

Several spectral bands may be considered for retrieving CH_4. Infrared measurements near 7.7 μm (e.g., Payne et al., 2009) generally lack sensitivity to near-surface CH_4, similar to MWIR CO. Both SCIAMACHY (e.g., Frankenberg et al., 2005; 2011, Wecht et al., 2014b) and GOSAT (e.g., Morino et al., 2011, Schepers et al., 2012) have produced CH_4 data products using reflected sunlight in the SWIR to obtain a true total column. CHRONOS will also measure a 2.2 μm SWIR CH_4 band, shown in Figure 6.

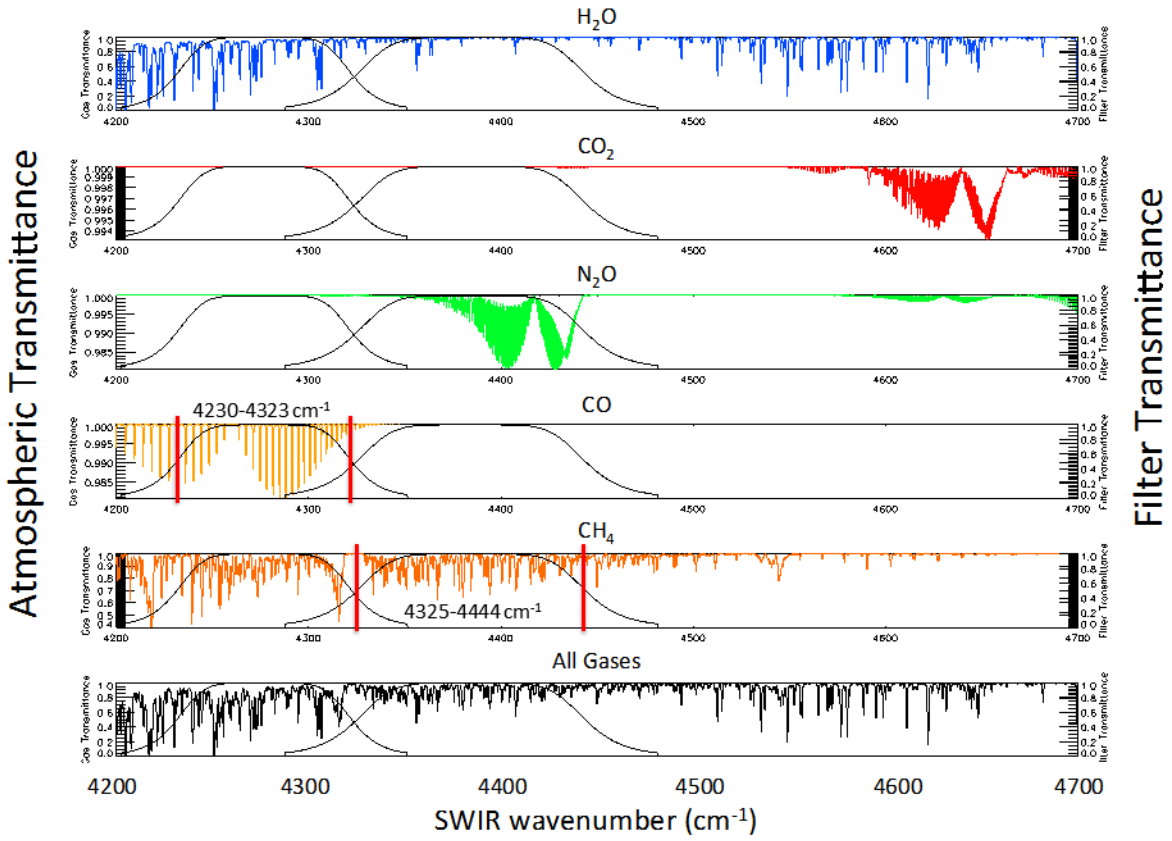

Figure 6: Atmospheric transmittance for primary trace gases in the SWIR vs. wavenumber. CHRONOS filter transmission is indicated by smooth bandpass curves with solid red lines at filter half-power points (50% transmittance). CHRONOS measures both CO and CH_4 in the SWIR.

The GFCR instrument generates band-integrated spectral radiance measurements through alternate gas and vacuum cells, producing radiance pairs. As shown in Figure 4, the Difference (D-signal), constructed by differencing the gas and vacuum cell radiances, contains spectral contributions only from the target gas absorption line positions within the spectral passband. The Average (A-signal), the mean of the gas and vacuum cell radiances, has a spectral contribution that is low at the target gas line positions and high elsewhere. As such, the A-signal carries background information on the FOV scene characteristics. To first order, the ratio of the D-signal and A-signal, D/A, eliminates the background radiance term and reduces the impact of uncertainties associated with surface reflectance, interfering gases, aerosols and clouds.

The designated pressure in the instrument cell determines the width of the fill-gas spectral lines, and thus the effective spectral sampling resolution of the correlation filter. We note that the

CHRONOS MWIR CO and SWIR CH_4 bands also contain water vapor (H_2O) and nitrous oxide (N_2O) absorption features (Figures 5 and 6). The gas correlation removes the absorption effects of these interfering gases for the D-signal. The interference of H_2O and N_2O in both the MWIR and SWIR channel A-signals is modeled in the forward model radiative transfer algorithm using analyzed H_2O concentration fields from meteorological data and inferred N_2O. N_2O is a long-lived gas (~120 years) with predictable variability (Angelbratt et al., 2011).

SCIAMACHY and GOSAT CH_4 SWIR retrievals are sensitive to scattering by dust, aerosols and thin cirrus (Gloudemans et al., 2008; Schepers et al., 2012) and address these errors by using CO_2 (with known abundance) as a proxy for the scattering effects or by performing a physical retrieval of effective parameters for the scattering layer. For GOSAT CH_4 data, these two approaches yield similar precision (~17 ppb) and biases less than 1% compared to TCCON (Wunch et al., 2010), but with lower bias for the proxy method (Schepers et al., 2012). In the proxy retrieval using CO_2, the dry mole fraction of CH_4 (x_{CH4}) is computed by $x_{CH4} = \frac{[CH4]}{[CO2]} x_{CO2}$ where $[CH4]$ and $[CO2]$ are the retrieved columns from spectral radiances that are close in wavenumber and x_{CO2} is the dry mole fraction computed from a global model of atmospheric CO_2 (Frankenberg et al., 2005; Schepers et al., 2012). This method assumes that aerosol scattering modifies the light path for CO_2 and CH_4 spectral absorption in the same way, and that model values for x_{CO2} are accurate.

Retrievals with GFCR measurements are similar to the "proxy retrieval" but they correct the input radiance instead of the retrieved column, and do not make assumptions about aerosol scattering in different spectral bands or rely on knowing CO_2 abundance. CHRONOS uses the D/A signal ratio where D and A are both modified in the same way by aerosol scattering, which has a smooth spectral behavior over the CHRONOS bandpass. This ratio gives an accurate total column amount, but to compute a dry mole fraction (xCH4), we require additional information about the surface pressure (for example, from GOES-16 meteorological data) in order to estimate the dry air column. In general, GFCR retrievals are more resilient than spectral radiance measurements to errors in surface and contaminant species assumptions due to the use of radiance differences and ratios (Pan et al., 1995).

3.3 Measurement Radiometric Accuracy and Precision

By using D/A signal ratios, the GFCR technique is inherently less sensitive to radiance bias errors than spectrometer measurements. However, three primary sources of potential retrieval bias remain: surface albedo spectral variability, aerosol scattering, and water vapor errors in meteorological data, which are typically < 10% for N. America (Vey et al., 2010). Spectral variation in surface albedo proved to be a significant obstacle for MOPITT CH_4 retrievals (Pfister et al., 2005). This was because of the width and spectral location of the MOPITT passband, combined with changing scene albedo arising from LEO spacecraft motion during the acquisition of a single measurement (Deeter et al., 2011). For CHRONOS, the CH_4 passband has been optimized in both width and spectral location (Table 1) to mitigate these errors.

For a GFCR, the radiance precision needed to measure a change in column is given by $\Delta D/A$, for D and A defined above, where ΔD is determined using the instrument sensitivity to the column change ($\partial D/\partial col$) (Pan et al., 1995). Profile or column retrieval precision requirements are achieved in ground processing by averaging geo-located, cloud screened radiances for three minutes (375 separate gas-vacuum measurements for each product: CO [4.6 μm, 800 hPa], CO [4.6 μm, 200 hPa], CO [2.3 μm, 100 hPa]; and 750 measurements of CH_4 [2.2 μm, 800 hPa]). A single retrieval for each product is performed on these averaged radiances. The process of averaging radiances and then retrieving products is repeated for all data acquired in the 9.7-minute data acquisition period. Table 1 lists the modeled signal-to-noise (SNR) and the total number of individual data acquisitions in each pixel in the 2D detector array ("frames") obtained in a single 9.7-minute data acquisition period, for the minimum radiance case defined from MOPITT on-orbit radiance records. This minimum SNR provides at least 30% margin for meeting the radiance precision requirements.

Table 1. The multi-layer dielectric optical coatings on the CHRONOS gas cell windows define the center wavelength and bandpass. Each spectral coating and cell pressure is identified through modeling to provide the optimal measurement. The signal-to-noise ratio (SNR) listed provides at least 30% margin over the SNR required to achieve radiance precision. All data frames are obtained within a single 9.7-minute data acquisition period.

Cell	Gas Filter	Center λ (μm)	Cell Pressure (hPa)	Band Pass (μm)	Band Pass (cm^{-1})	Co-added SNR at minimum radiance	Number of frames obtained
1	CO	4.6	200	4.562 – 4.673	2140 – 2192	595	95
2	Vacuum	4.6	0	4.562 – 4.673	2140 – 2192	--	--
3	CO	4.6	800	4.562 – 4.673	2140 – 2192	595	95
4	CO	2.3	100	2.313 – 2.364	4230 – 4323	3255	889
5	Vacuum	2.3	0	2.313 – 2.364	4230 – 4323	--	--
6	CH_4	2.2	800	2.250 – 2.312	4325 – 4444	4390	1012
7	Vacuum	2.2	0	2.250 – 2.312	4325 – 4444	--	--
8	CH_4	2.2	800	2.250 – 2.312	4325 – 4444	4390	1012

CO profile retrievals require 10% precision to capture the fine-scale space and time variability of CO and quantify transient sources (Fishman et al., 2012; Emmons et al., 2009). Based on GEO-CAPE CH_4 emission OSSEs (Wecht et al., 2014a), monthly emissions estimates with <10% error on county-level spatial scales (~40 km x 40 km) require a daily precision on averaged retrievals of total column CH_4 <1%. CHRONOS will deploy two identical CH_4 channels with combined 0.7% precision for a 9.7-minute data acquisition that exceeds the GEO-CAPE daily requirement. The CHRONOS sub-hourly CH_4 sampling capability and the relatively slow rate of change in CH_4 column abundance enable the combining of samples to further improve CH_4 column precision, allowing identification of CH_4 changes on daily scales, and verification of state and federal pollution reduction goals (Miller et al., 2013).As discussed in Section 3.2, a major advantage of the GFCR measurement technique is the ability to eliminate any contaminating signal that is not spectrally correlated with the lines of the cell target gas. In the spectral regions utilized by CHRONOS, water vapor spectral lines are ubiquitous, and in the SWIR, the effects of aerosol must be considered. Figure 7 shows CHRONOS simulated A and D signals for mid-latitude summer atmospheric conditions (Anderson et al., 1986), with and without aerosol scattering. The VLIDORT radiative transfer model (Spurr, 2006) is used for modeling the aerosol scattering, and the OPAC (Optical Properties of Aerosols and Clouds) database (Hess et al., 1998) provides AOD

adjusted to 2.25 μm. The case shown in Figure 7 is for AOD that is 50% larger than the OPAC urban aerosol case. Based on the simulated retrievals we perform, 1% errors in total column correspond to 0.2% errors in D/A. The nominal urban aerosol loading considered in OPAC would lead to ~ 0.026% errors in D/A, which translates to a ~0.13% error in total column. Similar errors in D/A due to aerosol scattering are obtained for the CHRONOS 2.3 μm CO channel, and can then be compared to MOPITT measurement errors in D/A that are around 1 to 2% for scenes with minimal geophysical noise. The insensitivity of D/A to aerosol scattering is found to hold for a large range of aerosol types and loading, with the largest errors (up to 0.3%) due to desert dust, consistent with Gloudemans et al. (2008). Expected errors due to uncertainties in water vapor were also simulated using perturbations of the mid-latitude summer atmosphere and are < 1% for CO and < 0.2% for CH_4.

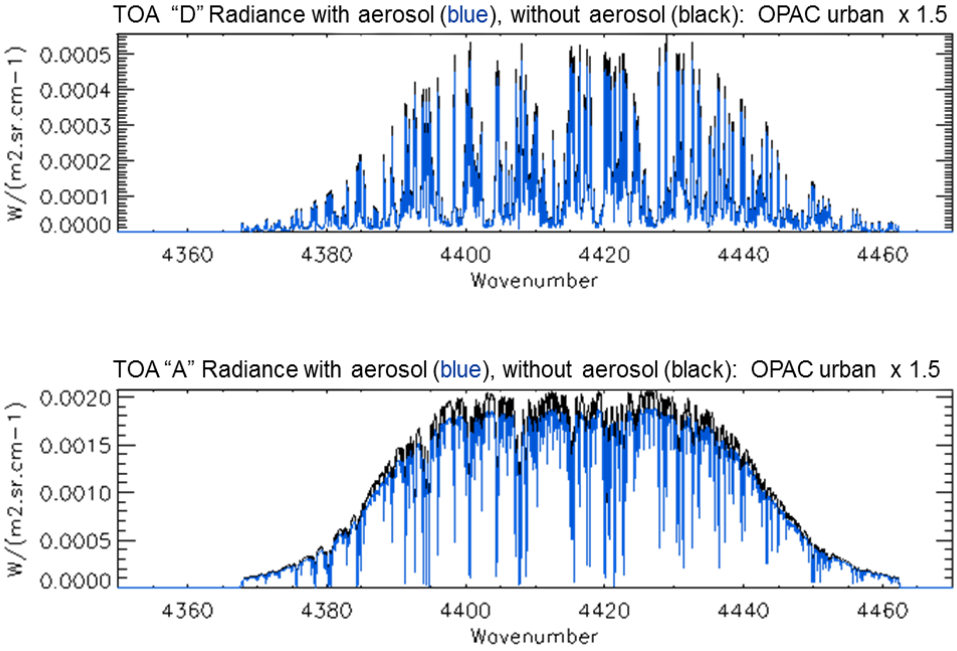

Figure 7: Forward model results with aerosol loading. Simulated radiance spectra for CHRONOS corresponding to TOA D (top panel) and A (bottom panel) signals with the CHRONOS CH_4 SWIR channel bandpass applied. Simulations are for a mid-latitude summer atmosphere with solar zenith angle = 0, satellite zenith angle = 40° and surface albedo = 0.2. Black lines represent the case without aerosol scattering and blue lines show radiances with aerosol scattering for urban aerosols (AOD is 0.089, which is obtained by scaling the OPAC urban aerosol case by 1.5). D/A is

computed after integration over the bandpass and is changed by -0.039% for the case with aerosols compared to without.

A summary of CHRONOS precision and accuracy requirements for column CO and CH_4 is given in Table 2. Validation activities for CHRONOS will use aircraft profiles from on-going flight programs, such as IAGOS (Nédélec et al., 2015) and existing ground data networks such as TCCON (Wunch et al., 2010) to detect biases in CO and CH_4 similar to the proven approach used for GOSAT and OCO-2 validation (Schepers et al., 2012).

Table 2. Expected precision and accuracy for CHRONOS.

Column Error Source	MWIR CO (night)	MWIR+SWIR CO (day)	SWIR CH_4 (day)
Precision requirement	<10%	<10%	<0.7%
MOPITT performance	5-15%	2-10%	n/a
Corresponding SNR (A/ΔD)	457	2499	3374
Radiometric bias	<0.1%	<0.1%	<0.1%
10% water vapor error	<0.7%	<0.7%	<0.15%
Albedo variation	Negligible for MWIR CO band[1]	<0.06%	<0.1%
Urban aerosol loading	Negligible in MWIR[2]	<0.03%	<0.13%

[1](MWIR CO band is 0.11 μm wide; based on MOPITT experience, no significant errors due to albedo spectral variation); [2](e.g., Russell et al., 1999, Bohren and Huffman, 1983)

4 The CHRONOS Instrument and Operation

The CHRONOS measurement domain, shown in Figure 8, extends over North America and includes adjacent oceans in order to observe pollution inflow and outflow using observations in the MWIR CO channels. In the SWIR channels, sunlight is mostly absorbed in the ocean, and no trace gas retrievals are expected over the ocean in the SWIR channels. The CHRONOS ground sample area varies gradually across the field of view due to curvature of the Earth as seen from GEO, with smaller than 4 km x 4 km (16 km^2) nominal pixel area at the center of the domain, increasing to 19.3 km^2 at the edge of the CONUS domain (e.g., Seattle). This spatial resolution enables emissions estimates at the U.S. county scale even for the smallest county in the continental U.S., New York County (i.e., Manhattan), NY, which contains 3.5 CHRONOS pixels. The increase

in pixel size toward northern latitudes is commensurate with the increasing scale of dominant emissions sources, such as large-scale wetlands in Canada (e.g., Pickett-Heaps et al., 2011). To account for these variations, CHRONOS Level 2 (individual retrieval) data will be re-gridded (Vijayaraghavan et al., 2008; Guizar-Sicairos et al., 2008) in Level 3 (gridded) data to facilitate user scientific analysis using standard tools.

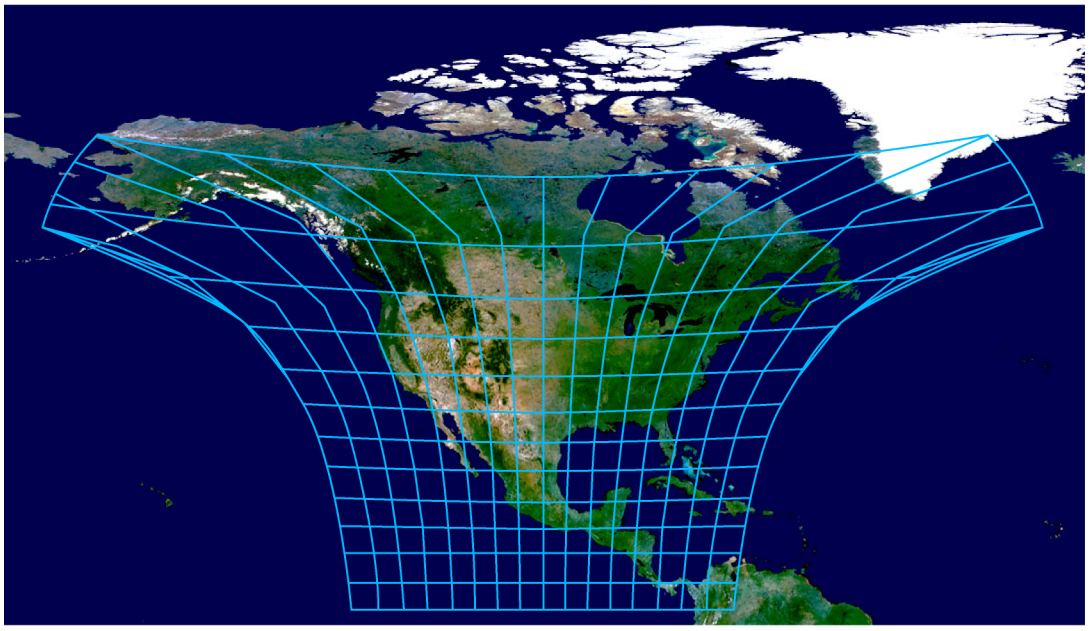

Figure 8: CHRONOS field of view from geostationary orbit at 100° W. Each grid cell above represents 125 x 125 pixels. All pixels are acquired with full precision within the ~10 minute CHRONOS data acquisition.

The CHRONOS GFCR is a staring infrared 2-D camera with a continuously rotating wheel that houses gas and vacuum cells, which sequentially pass through the optical path. Figure 9 depicts the instrument, which comprises optomechanical, calibration, focal plane, thermal, and control electronics subsystems. Within the optomechanical subsystem, the gas cell filter wheel assembly contains cells as specified in Table 1. A selection mirror determines the source of the input radiance being filtered by the cells and imaged by the optics (Earth view, on-board calibration subsystem, a deep space view, and a blocked or closed position).

CHRONOS uses an all-digital (Brown et al., 2010) cryogenically cooled HgCdTe large area focal plane array to detect the spectral radiance. The CHRONOS instrument has been designed around commercially available, space proven, radiation-hardened large format focal plane arrays (e.g.,

515 flown on India's Chandrayaan-1 mission/NASA Moon Minerology Mapper (Green et al., 2011), DOD's CHIRP experiment (Levi et al., 2011), and NASA's Near Infrared Camera on the James Webb Space Telescope (Garnett et al., 2004)). Low dark current (6.2×10^9 e-/cm^2-s at 110 K), low readout noise (high gain: 40 e- rms; low gain: 200 e- rms), high, stable quantum efficiency (0.7 at 2.2, 2.3, and 4.6 μm) and fast electronics are necessary characteristics for this application. For a
520 2-D imager such as CHRONOS, the pixel format (presently 2048 x 2048) and the desired observational domain determine the single pixel ground sample area from geostationary orbit.

A small, high-reliability, space-proven cryocooler cools the focal plane array and a portion of the optics module. Instrument control electronics provide the functionality to receive communications (commands) from the host spacecraft, control the instrument, sequence the data collection
525 operations, and ultimately send science data to the host for downlink.

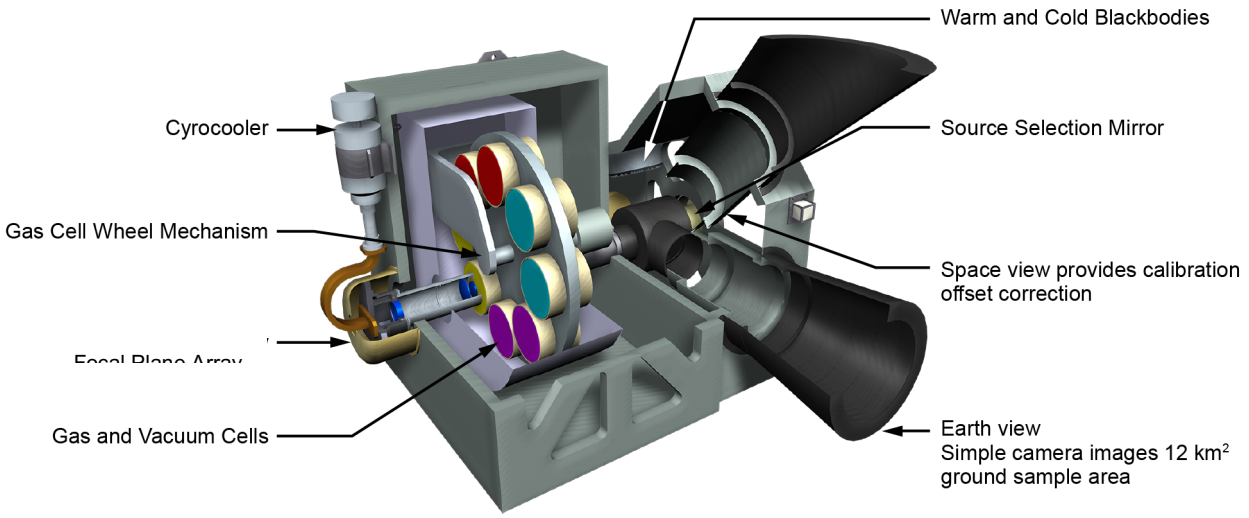

Figure 9: The CHRONOS GFCR is a staring infrared camera with gas cell filters in the optical path. A source selection mirror determines the input to the system (Earth FOV, one of three onboard calibration sources, deep space, or closed). Optics image this source input onto a
530 cryogenically cooled large area focal plane array.

Figure 10 shows the image collection timing between a gas cell and its physically adjacent paired vacuum cell on a continuously rotating wheel. When an unobscured FOV emerges as a cell rotates through the optical path, the focal plane collects an image of the entire physical domain using one
535 of two integration times (corresponding to low gain and high gain). Multiple gains are necessary to image the high dynamic range across the entire FOV with the required signal-to-noise ratio

(SNR). Only 60 msec later, the FOV of the next cell, (a vacuum cell in the case of Figure 10), is unobscured and the focal plane collects an image. The short 60 msec between images effectively freezes the scene, allowing the GFCR algorithm to process the pair cell and vacuum signals together without geometric corrections, and providing nearly simultaneous gas and vacuum cell views described in Section 3.1. Single frames of paired gas and vacuum cell signals, as described above, are continuously collected until a prescribed number of images have been collected for each gas/vacuum cell pair. All of the images are downlinked through the host spacecraft. In ground processing, the single frame Level 0 (signal count) data are processed for image registration and radiance calibration before being co-added to build up the required signal to noise ratio for the Level 1 (radiance) measurement at each location (pixel). The full data collection sequence includes calibration views, the full Earth view image collection outlined above for both low and high gains, followed again by calibration. The required SNRs for all channels are achieved in 9.7 minutes of measurement time. The CHRONOS gas cell filter wheel rotates continuously, and data may be obtained continuously, for up to 6 full-precision data takes per hour. Parameter tables can be uploaded to alter this sequence, or command additional data collects as necessary.

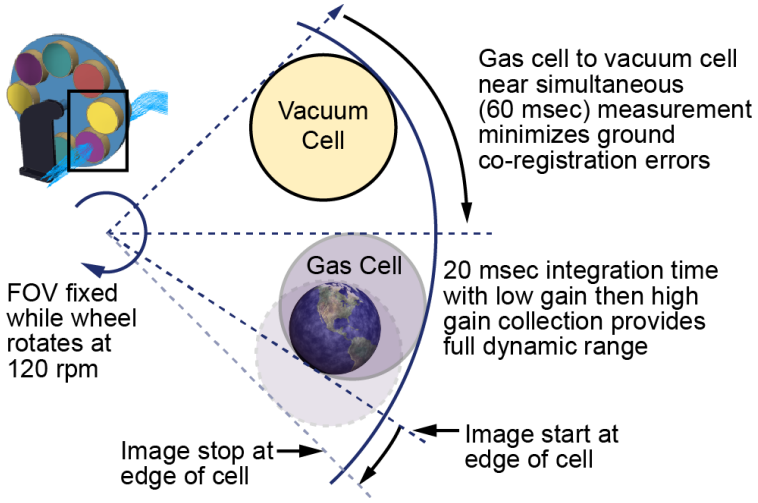

Figure 10: CHRONOS' eight gas cells are mounted in a continuously spinning mechanism wherein each cell in sequence exposes an unobscured Earth FOV as defined in Figure 8. A single frame image is collected with a prescribed integration time. Single frames are continuously collected and downlinked via the host spacecraft. In ground processing the ensemble of single frames are co-added to achieve the required signal to noise ratios for each measurement.

For on-orbit radiance calibration, CHRONOS views high-precision hot and cold black bodies and deep space for the MWIR channels, and a tungsten lamp (LandSat Operational Land Imager heritage) and a closed aperture for the SWIR calibration within each 10-minute data acquisition.

CHRONOS cloud detection will follow the MOPITT algorithm approach, which uses the MWIR A-Signals as the primary test for the presence of cloud, based on observed brightness temperature (Warner et al., 2001). In the case of MOPITT operation, cloud flags are then verified with the Moderate Resolution Imaging Spectroradiometer (Terra/MODIS) cloud data products, when available. Using a similar approach, CHRONOS will use the GOES-R Advanced Baseline Imager (ABI) cloud mask (Heidinger, 2011) to verify cloud detection. Cloud movement is assumed negligible during a 60 msec frame measurement. MOPITT retrieval experience shows that the GFCR technique can tolerate up to ~5% cloud contamination and still treat the pixel as cloud-free (Warner et al., 2001). While the approach of using D/A for retrievals discussed in Section 3.3 will cancel some of the errors due to undetected aerosols or clouds (e.g., thin cirrus), remaining retrievals errors (e.g., O'Dell et al., 2011), particularly for CH_4, will require further study using both CHRONOS radiances and GOES-16 ABI observations. Combined with CHRONOS' sub-hourly revisit, the small nominal ground sample area increases the probability of obtaining cloud-free pixels in regions of broken cloud. This is an advantage compared to observations from LEO where a cloud-free scene may not be encountered at a given location over several days. Figure 11 shows OSSE results for simulated CHRONOS observations over a 2-week summer period. This study indicates that 70–75% of 4 km x 4 km pixels can be treated as cloud-free in the West and Central U.S. and 60–65% in the East U.S.

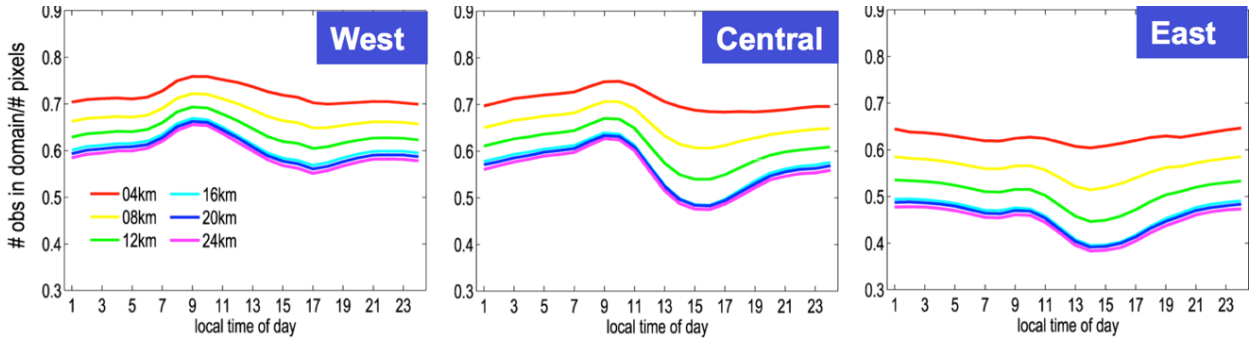

Figure 11: CONUS cloud statistics from OSSE results for 15-30 July 2006 using a high spatial resolution WRF-Chem run and a GFCR instrument with allowable pixel cloud fraction set at 3%. For different geographical regions, the fraction of cloud-free scenes (the number of cloud-free

pixels observed as a fraction of the total number of pixels in the region) is plotted for different assumed pixel sizes; red represents the CHRONOS 4 km x 4 km pixels. Clouds are defined by 4-
585 km grid integrated total hydrometeors > 10^{-8} kg/kg.

After cloud detection, the retrieval algorithm accesses current best meteorological analysis data for surface pressure and temperature, atmospheric temperature and water vapor profiles to include in the forward model radiance calculation. Optimal estimation (Rodgers, 2000) is then used to
590 convert Level 1 TOA radiances to Level 2 vertical trace gas distributions.

5 Characterization of CHRONOS CO and CH_4 Retrievals

5.1 Multi-spectral CO Measurements and Vertical Profile Information

CHRONOS CO measurements use MWIR thermal emission (day and night), with sensitivity to free tropospheric CO, and SWIR solar reflection (day), with sensitivity to total column CO. These
595 measurements are combined in a multispectral retrieval to obtain vertical profiles of CO abundance, Figure 12. Following MOPITT retrieval algorithms, CHRONOS will employ the optimal estimation methods of Rodgers (2000), which provide an averaging kernel (AK) that represents the sensitivity of the retrieval to the abundance of the target trace gas in each retrieval pressure layer. Degrees of freedom for signal (DFS) in the retrieval are computed from the trace
600 of the AK, and provide a measure of the independent profile information available. DFS values are ~1.5 to 2 for retrievals using only MWIR channels with CO gas cells at two different pressures, while a column retrieval with the SWIR channel alone has at most a DFS of 1. The CHRONOS multispectral retrievals have DFS values typically > 2. Figure 13 shows CO retrieval results from MOPITT that compare the sensitivity of MWIR-only, SWIR-only and multispectral retrievals. We
605 note that MOPITT retrievals would have higher values of DFS without the presence of geophysical noise in MOPITT observations (Deeter et al., 2011). Geophysical noise is introduced by changes in the FOV surface albedo due to LEO spacecraft motion during the time taken for MOPITT signal acquisition. The CHRONOS stationary FOV and single frame integration time of 20 msec mitigates this source of noise. Multispectral CO retrievals from MOPITT have demonstrated the
610 improvements in sensitivity to surface layer CO abundance (Worden et al., 2010), have been validated (Deeter et al., 2011; 2013), and used in many studies to distinguish surface pollution

emissions from transported plumes (e.g., Worden et al., 2012; Jiang et al., 2013; 2015; He et al., 2013; Silva et al., 2013; Worden et al., 2013; Huang et al., 2013; Anderson et al., 2014; Bloom et al., 2015). The CHRONOS multispectral retrievals would extend the MOPITT record of vertical layers of CO over North America when MOPITT is finally decommissioned, since MOPITT is the only satellite mission to demonstrate multispectral trace gas retrievals from a single space-based instrument. The multispectral retrieval approach for CO allows for up to 3 DFS, which is a practical upper limit on CO vertical information based on atmospheric radiative transfer. As has been demonstrated by other on-orbit sensors measuring CO, an instrument design with more gas cells, or a spectrometer with arbitrarily fine spectral resolution (George et al., 2009), does not produce retrievals with greater DFS. Thus, CHRONOS would produce the maximum vertical information possible for CO with a passive sensor.

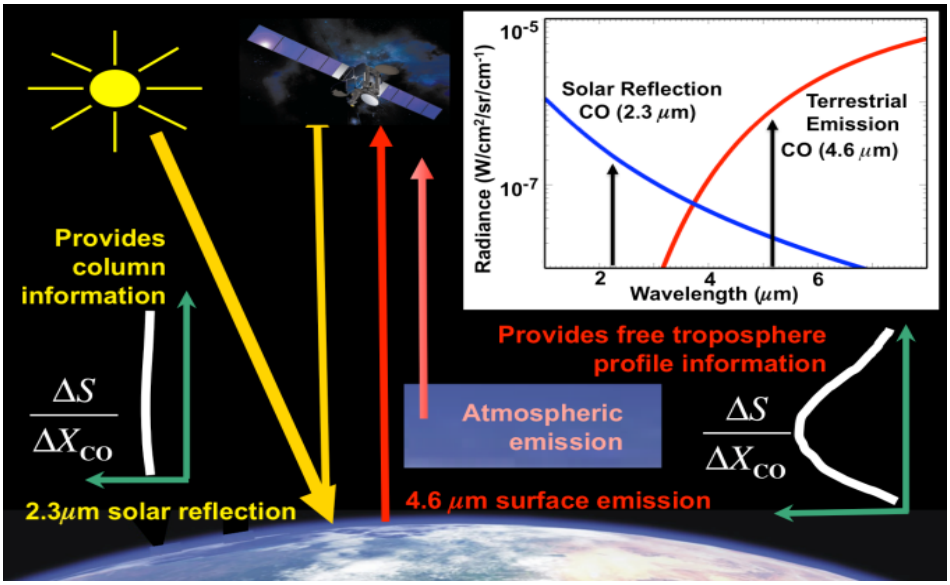

Figure 12: Physics of CHRONOS and MOPITT multispectral measurements. In the SWIR at 2.2 and 2.3 μm, measurement signals rely on daytime reflected solar radiation and weak spectral features. Changes in CH_4 and CO mixing ratios, ΔX, produce uniform signal sensitivity, ΔS, throughout the vertical profile, including near the surface. In the MWIR at 4.6 μm, signal sensitivity is greatest in the middle troposphere, except in cases of high thermal contrast between the surface and the lowest atmospheric layers. CHRONOS CH_4 SWIR retrievals use the solar reflected radiance to provide a true total column, and CO multispectral retrievals combine the SWIR and MWIR measurements to increase the sensitivity to near-surface CO. While this

increased sensitivity varies depending on scene characteristics such as albedo, in many cases, it provides improved information to distinguish local air pollution emissions and transported plumes.

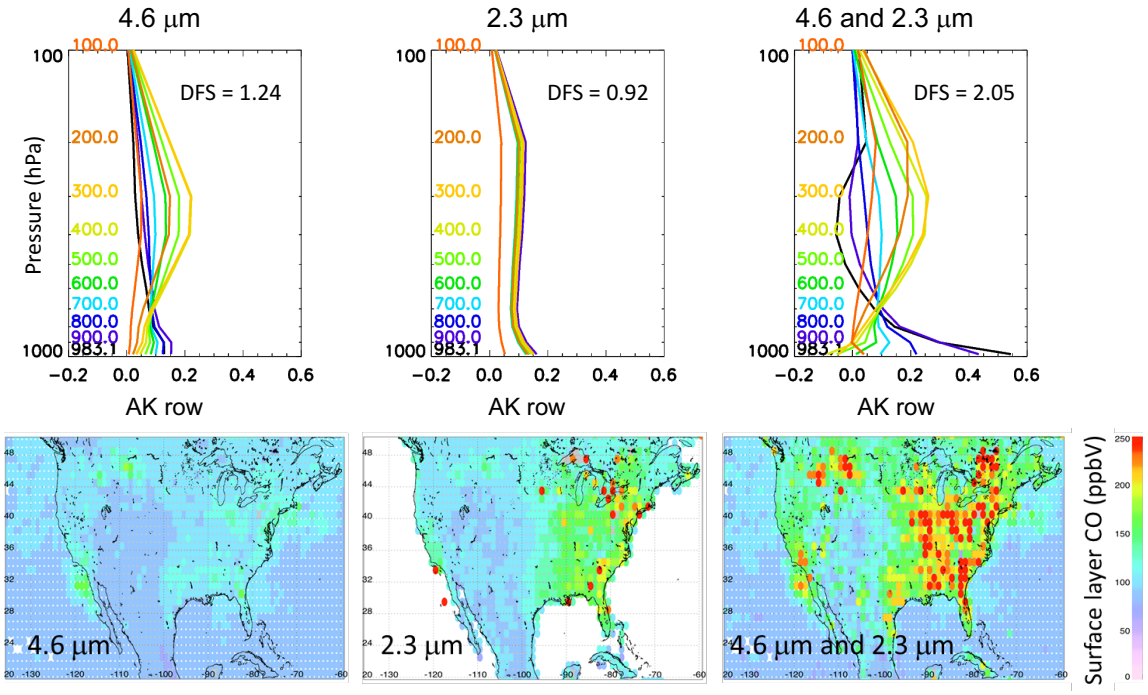

Figure 13: Comparison of surface layer CO for MOPITT MWIR (4.6μm), SWIR (2.3 μm) and multispectral (MWIR and SWIR combined) retrievals for Aug. 2000. Top panels show representative averaging kernel (AK) rows, where line colors indicate the pressure layers given on the left side of the panels, for the three retrieval types (location at 30.72°N, 96.50°W). Bottom panels show maps of the surface layer CO abundance indicating how detailed information is obtained in the multispectral retrievals, but is absent in the single channel retrievals.

5.2 Retrieval Sensitivity to Near-Surface CH_4

The vertical profiles of CH_4 are similarly characterized using the AK from optimal estimation retrievals (Rodgers, 2000). Radiative transfer modeling has been developed to compute weighting functions, i.e., radiance Jacobians integrated over the filter bandpass to assess the sensitivity to changes in the CH_4 column. Figure 14 shows an example of a simulated CHRONOS CH_4 weighting function and corresponding AK (see caption for simulation assumptions). For the SWIR

measurements, the signal source is solar reflectance with a measurement sensitivity response that is nearly uniform in the vertical, giving true total column CH_4 information with DFS close to 1.

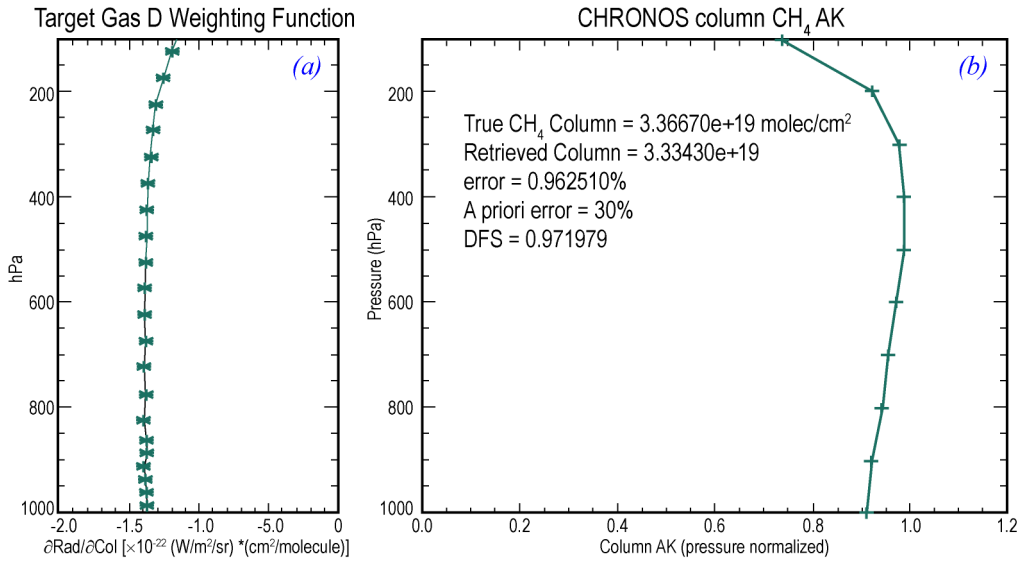

Figure 14: CHRONOS CH_4 D-signal weighting function and retrieval column AK. (a) Sensitivity of the D-signal to changes in CH_4 column ($\partial \mathrm{Rad(D)}/\partial \mathrm{col}$) as a function of vertical pressure for a standard mid-latitude summer atmosphere with albedo = 0.1, SZA = 0°, satellite ZA = 40°. (b) The retrieval column averaging kernel from the corresponding D/A signal ratio and Jacobian. This assumes CHRONOS measurement precision and a priori covariance with 30% diagonal errors and 500 hPa correlation length, (retrieval was performed on a coarser pressure grid than the weighting function calculations). Since the signal source is solar reflectance, the response is nearly uniform vertically with DFS close to 1.

The magnitude and shape of the column CH_4 AKs have only small variations with input atmospheric parameters (such as temperature and water vapor) and input surface parameters such as albedo (assuming non-zero albedo). However, there is a more significant dependence of the CH_4 AK on parameters that depend on the total amount of CH_4 along the observation path, such as solar zenith angle (SZA), satellite zenith angle and CH_4 abundance. Figure 15 shows how the sensitivity to CH_4 in the lowest (near-surface) layer depends on SZA for A, D and D/A signals. While the A and D signals both have reduced sensitivity with higher SZA, as expected for solar reflection radiances, the D/A ratio sensitivity increases slightly, with relatively uniform response, for daylight hours. Figure 16 shows the dependence of CH_4 AKs on SZA and CH_4 total column,

with sensitivity to surface CH_4 that increases with increasing values, especially for SZA, as expected from Figure 15.

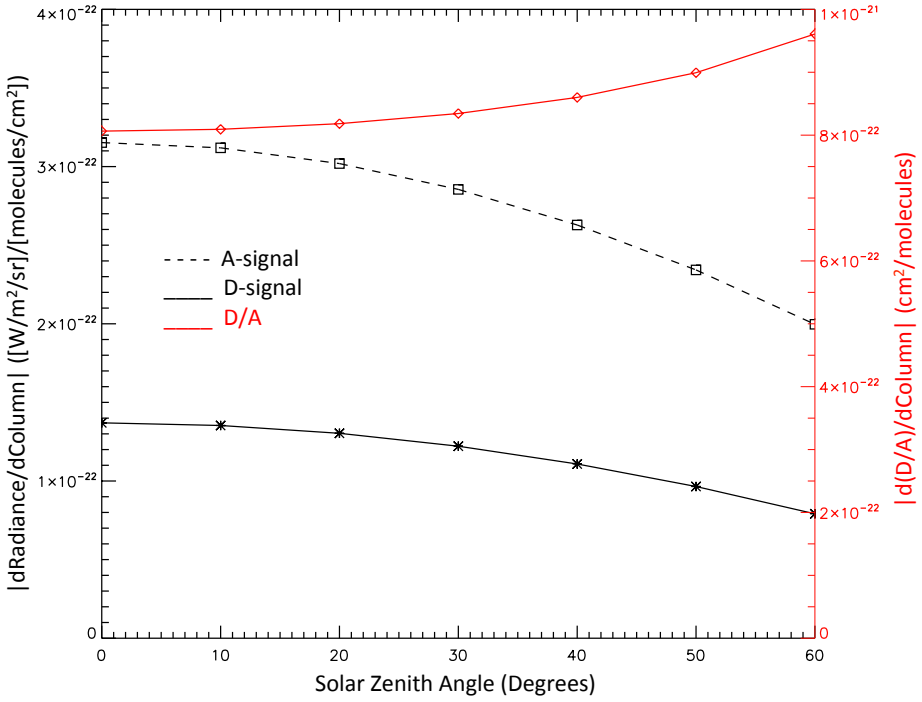

Figure 15: Variation of CHRONOS sensitivity to surface CH_4 with solar zenith angle (SZA). Absolute values for the surface layer CH_4 Jacobians are plotted for the A-signal, D-signal and D/A ratio as a function of SZA.

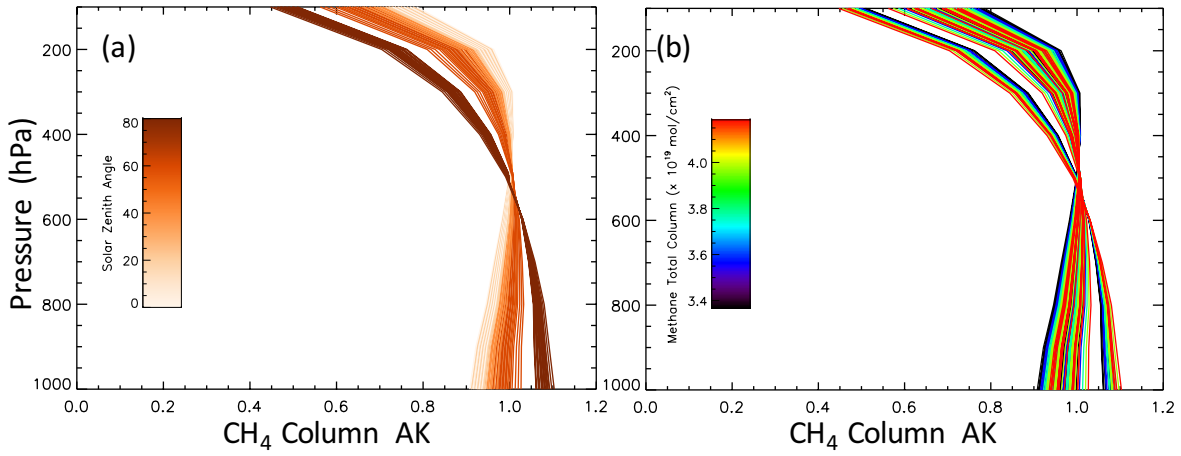

Figure 16: Variation of CHRONOS CH_4 averaging kernels for different SZA (left) and CH_4 total column (right) for 100 simulations with different SZA and CH_4 column values. Within each "group" of SZA values, the lesser AK dependence on low-to-high values of CH_4 can be seen.

6 Relationship of CHRONOS to Current and Future Missions

CHRONOS addresses key NASA science goals and National Research Council Decadal Survey questions with heritage from past satellite instruments and opportunities for synergistic observations with current and upcoming LEO and GEO platforms. In particular, CHRONOS would complement planned NASA missions for air quality and carbon cycle science. It would deliver air pollutant measurements identified in the 2007 Decadal Survey GEO-CAPE mission (NRC, 2007) and address currently unmet science objectives described in the GEO-CAPE Science Traceability Matrix (Fishman et al., 2012).

6.1 Other Satellite CO Observations

Along with MOPITT, satellite measurements of CO in the MWIR (4.6 μm) are available from AIRS, a grating spectrometer on EOS-Aqua launched in 2002 (Auman et al., 2003); the IASI FTS instruments on MetOp-A, B and C, launched in 2006, 2012 and expected in 2018 (Crevoisier et al., 2014); and the CrIS FTS instruments on Suomi NPP, launched 2011, and JPSS1-4 with projected launches starting in 2017 (Gambacorta et al., 2014). These LEO observations give daily global coverage at morning (IASI) and afternoon (AIRS, CrIS) equator crossings with sensitivity to CO in the middle troposphere for most observing conditions (George et al., 2009). The measurements are expected to be available during the CHRONOS mission time frame, and will provide valuable intercomparisons for the MWIR CHRONOS CO channel.

TROPOMI, a UV-VIS-NIR-SWIR spectrometer, launched in October 2017, provides daily global coverage from LEO at a 13:30 equator crossing with 7 km x 7 km spatial resolution and 10% column precision and 15% accuracy for SWIR (2.3 μm) CO observations (Veefkind et al., 2012). The TROPOMI CO measurements will provide true total column CO retrievals with more spatial coverage than MOPITT, but will not have MOPITT's CO vertical profile information. GOSAT-2 (http://www.gosat2.nies.go.jp), with expected launch in 2018, will also measure SWIR CO bands but with measurements spaced around 200 km apart and large gaps in the ground sampling. CHRONOS multispectral CO measurements could provide vertical profiles of CO over the continental U.S. domain every 10 minutes, along with total column CO that can be compared to TROPOMI and GOSAT-2. The LEO observations of CO outside of the CHRONOS field of regard would be useful for constraining CO transported from sources outside North America.

NASA selected the GeoCARB mission in November 2016, with capability to measure CO in one spectral region (Polonsky et al. 2014; Kumer et al., 2013) and primary carbon cycle science objectives unrelated to air pollution transport. Compared to the CHRONOS requirement for CO measurement in two spectral regions, this GeoCARB limitation to CO in one spectral region precludes GeoCARB from evaluating vertical pollution transport, or providing the test of these atmospheric motions as calculated by models (NAS, 2017). Both Polonsky et al. (2104) and Kumer et al. (2013) describe mission descopes that eliminate GeoCARB measurements of CO entirely if needed to ensure success for GeoCARB CO_2 and solar induced fluorescence science objectives.

6.2 Other Satellite CH_4 Observations

GOSAT, launched in 2009, measures CH_4 from LEO in the SWIR (1.6 μm), with relatively sparse coverage, a 10-km diameter footprint and column precision around 0.6% for single observations (Schepers et al., 2012). Improved sampling, coverage and precision are expected for GOSAT-2. Wecht et al. (2014a) show that hourly GEO SWIR CH_4 observations over California with 4 km x 4 km spatial resolution and 1.1% precision provide about 20 times the information for estimating CH_4 emissions compared to 3 days of GOSAT observations. This means that one 10-minute collection of CHRONOS data would provide more information than a year of GOSAT observations, assuming $1/\sqrt{N}$ improvement for 365 days. Turner et al. (2015) used 3 years (2009-2011) of GOSAT CH_4 measurements to estimate North American emissions with 1/2° x 2/3° (~50 km x 70 km) spatial resolution, and found significant differences with the a priori inventory for anthropogenic emissions. Assuming the same information scaling found by Wecht et al. (2014a), CHRONOS would be able to quantify CH_4 emissions for this spatial scale on a daily basis, with the capability to assess more rapid emission changes for events such as the 2015 Aliso Canyon gas leak (Conley et al., 2016).

TROPOMI in LEO uses near infrared (NIR) 0.76 μm and SWIR (2.3 μm) bands for CH_4 measurements and has an expected 0.6 % precision for single column CH_4 retrievals at 7 km x 7 km spatial resolution (Butz et al., 2012). Based on an analysis in Jacob et al. (2016), TROPOMI should be capable of regional scale quantification of CH_4 emissions. The daily probability of viewing sources that are either transient or obscured by clouds would be higher for CHRONOS in GEO than for TROPOMI, since CHRONOS could observe the entire continental U.S. domain six

times during each daylight hour. CHRONOS also has a higher probability of cloud-free observations given its smaller pixel size (see Figure 11).

GeoCARB describes CH_4 measurements in the SWIR (2.3 μm) region with 1% precision three times per day at 5 km x 5 km spatial resolution (O'Brien et al., 2016), although earlier studies (Kumer et al., 2013) explored CH_4 measurements at 1.65 μm. GeoCARB's more frequent CH_4 observations than TROPOMI may provide for similar precision in a smaller spatial footprint than TROPOMI. CHRONOS could observe CH_4 as often as every 10 minutes in daylight with 0.7% precision and 4 km x 4 km resolution. These frequent CHRONOS CH_4 measurements could be co-added to improve hourly precision, or used to examine anthropogenic source evolution over time.

For emissions on a 1/2° x 2/3° grid, Wecht et al. (2014a) show that GEO-CAPE SWIR CH_4 hourly observations (assuming 1.1% column precision) have 2.4 times the information of daily TROPOMI for estimating CH_4 emissions. More work is needed using OSSEs to understand how to optimally exploit LEO observations of CH_4 and CO, especially from TROPOMI and GOSAT-2, in combination with the information on diurnal variability that CHRONOS could provide. This extends to examination of the North American carbon budget since CO and CH_4 measurements from CHRONOS, in conjunction with detailed CO_2 observations from planned and operating missions, would allow differentiation of anthropogenic combustion and wildfire sources of CO_2.

Missions with the ability to measure "true" columns for CO and/or CH_4 (i.e., using SWIR spectra for the measurement) are summarized in Table 3. Note that for CHRONOS, 10% precision on CO observations meets the GEO-CAPE CO precision requirement of 10 ppbv. The CHRONOS 0.7% precision for CH_4 observations is achieved in a single 9.7-minute data collection; improved precision can be achieved by combining multiple data collections.

Table 3: Relationship of CHRONOS to current and future CO and CH_4 missions. CHRONOS contributes unique observations of multispectral CO for tracing air pollution transport, and temporally dense CH_4 observations to improve emissions estimates across a continental domain.

Instrument	MOPITT	TROPOMI	TANSO-FTS-2	Sentinel-5/UVNS	GeoCARB	CHRONOS
Instrument type	Gas Filter Correlation Radiometer	Grating Spectrometer	Fourier Transform Spectrometer	Grating Spectrometer	Grating Spectrometer	Gas Filter Correlation Radiometer
Spacecraft	NASA Terra	ESA Sentinel-5P	GOSAT-2	METOP SG A1	Commercial	Proposed
Launch Date	1999	2017	2018	2021	2022	NET 2024
Source of Info	(Drummond, et al., 2010)	ATBD, (Veefkind, et al., 2012)	(Matsunaga et al., 2017)	(Ingmann, et al., 2012)	(O'Brien, et al., 2016)	This Work
Orbit	LEO SSO	LEO SSO	LEO SSO	LEO SSO	GEO	GEO
Domain	Near Global	Near Global	Near gobal	Near Global	North/South America	North America
Pixel Size, km^2	22 x 22	7 x 7	9.7 x 9.7	7.5 x 7.5	5 x 5	4 x 4
Revisit	3 days	Daily	6 days	Daily	3x/day	Sub-hourly*
CH_4 Spectral Region, μm	2.222-2.293	2.303-2.385	1.563-1.695 5.56-8.45	1.590-1.675	2.301-2.346	2.250-2.313
CH_4 Column Precision, %	-	0.6	0.6	1	0.6	0.7
CO Spectral Regions, μm	2.323-2.345	2.303-2.385	1.923-2.381	2.305-2.385	2.301-2.346	2.313-2.364
	4.562-4.673	-	-	-	-	4.562-4.673
CO Column Precision, %	10	10	10	10	10	10

*** up to 6 observations per hour**

7 Conclusions

We report a new capability for space based measurements of the important air pollutants carbon monoxide (CO) and methane (CH_4) as often as six times per hour. CO and CH_4 abundance are chemically linked in Earth's atmosphere as the principal sinks of hydroxyl. Sub-hourly observations of CO abundance, which is highly variable in space and time, can reveal new knowledge of the vertical and horizontal transport of air pollution. When sub-hourly observations of more slowly varying CH_4 abundance are combined, the temporally dense observations can significantly improve the precision of CH_4 emissions estimates. Observing System Simulation Experiments reported elsewhere show that improved CO and CH_4 emissions estimates can improve air quality forecasts that protect public health.

The CHRONOS investigation using 2-D imaging with full spectral resolution, would contribute the only sub-hourly CO and CH_4 observations for the U.S. component of an international GEO satellite constellation for atmospheric composition (CEOS, 2011) that includes the ESA/EUMETSAT Sentinel 4 mission over Europe and the Korean MP-GEOSAT/GEMS over Asia, along with the NASA TEMPO mission. LEO components (Sentinel 5/UVNS, TROPOMI, GOSAT-2) of the constellation provide the global context (Table 3) for CHRONOS observations in assessing regional-to-global emissions and transport.

The main points defining the CHRONOS science investigation may be summarized as follows:

1. CHRONOS would deliver the first sub-hourly observation capability for comprehensive U.S. CH_4 and CO emission inventories and the ability to distinguish local from transported air pollution.
2. At the county scale, CHRONOS would enable new estimates of rapidly changing, highly variable CH_4 and CO emissions from growing natural gas extraction and increasingly frequent and severe wildfires. These emissions estimates are essential for air quality, climate, and energy management decisions.
3. The dense data from sub-hourly air pollution observations at fine spatial resolution (nominally 4 km × 4 km) over the entire greater North American domain would quantify diurnal changes in air pollution and discriminate different source regions for urban and rural emission activities.
4. CHRONOS' multispectral CO retrieval would provide vertical information near the surface in addition to the free troposphere to distinguish local air pollution from transported air pollution through horizontal and vertical tracking.
5. CHRONOS observations would strengthen the international air quality satellite constellation.

These science goals would be achieved by taking advantage of a simple, low-risk instrument design that is well suited to the CHRONOS CO and CH_4 measurements. The GCFR heritage follows the successful 17-year, on-orbit operation of MOPITT over a wide range of observing conditions. This technique provides for high effective spectral resolution for the target gases, high signal levels compared to other types of spectrometers with similar spectral sensitivity, and small impact from signals due to interfering gases, aerosols, clouds and changing scene.

Acknowledgements

This work was partly supported by NASA grant NNX15AK98G. The National Center for Atmospheric Research (NCAR) is sponsored by the National Science Foundation. The NCAR MOPITT project is supported by the NASA Earth Observing System Program. We thank Glenn Diskin and the DACOM measurement team at NASA Langley for providing the DISCOVER-AQ CH_4 measurements shown in Figure 3.

References

Abatzoglou, J. T. and Williams, A. P.: Impact of anthropogenic climate change on wildfire across western US forests, Proceedings of the National Academy of Sciences of the United States of America, doi:10.1073/pnas.1607171113, 2016.

Acton, L. L., Griggs, M., Hall, G. D., Ludwig, C. B., Malkmus, W., Hesketh, W. D., and Reichle, H.: Remote measurement of carbon monoxide by a gas filter correlation instrument, AIAA Journal, 11 (7), 899–900, 1973.

Allen, D. T., Torres, V. M., Thomas, J., Sullivan, D. W., Harrison, M., Hendler, A., Herndon, S. C., Kolb, C. E., Fraser, M. P., Hill, A. D., and Lamb, B. K.: Measurements of methane emissions at natural gas production sites in the United States, Proceedings of the National Academy of Sciences of the United States of America, 110 (44), 17768–17773, doi: 10.1073/pnas.1304880110, 2013.

Anderson, G. P., Clough, S. A., Kneizys, F. X., Chetwynd, J. H., and Shettle, E. P.: AFGL atmospheric constituent profiles (0–120 km), AFGL-TR-86-0110, AFGL(OPI), Air Force Geophysics Laboratory, Hanscom Air Force Base, MA 01736, USA, 1986.

Anderson, D. C., Loughner, C. P., Diskin, G., Weinheimer, A., Canty, T. P., Salawitch, R. J., Worden, H. M., Fried, A., Mikoviny, T., Wisthaler, A., and Dickerson, R. R.: Measured and modeled CO and NOy in DISCOVER-AQ: An evaluation of emissions and chemistry over the eastern US, Atmospheric Environment, 96, 78–87, doi:10.1016/j.atmosenv.2014.07.004., 2014.

Angelbratt, J., Mellqvist, J., Blumenstock, T., Borsdorff, T., Brohede, S., Duchatelet, P., Forster, F., Hase, F., Mahieu, E., Murtagh, D., Petersen, A. K., Schneider, M., Sussmann, R., and Urban, J.: A new method to detect long term trends of methane (CH_4) and nitrous oxide (N_2O) total columns measured within the NDACC ground-based high resolution solar FTIR network, Atmospheric Chemistry and Physics, 11, 6167–6183, doi:10.5194/acp-11-6167-2011, 2011.

Arellano, A. F., Hess, P. G., Edwards, D. P., and Baumgardner, D.: Constraints on black carbon aerosol distribution from Measurement of Pollution in the Troposphere (MOPITT) CO, Geophysical Research Letters, 37 (17): doi:10.1029/2010gl044416, 2010.

Aumann, H. H., Chahine, M. T., Gautier, C., Goldberg, M. D., Kalnay, E., McMillin, L., M., Revercomb, H., Rosenkranz, P. W., Smith, W. L., Staelin, D. H., Strow, L. L., and Susskind, J.: AIRS/AMSU/HSB on the Aqua mission: Design, science objectives, data products, and processing systems, IEEE Transactions on Geoscience and Remote Sensing, 41 (2), 253–264, 2003.

Barth, M. C., Lee, J., Hodzic, A., Pfister, G., Skamarock, W. C., Worden, J., Wong, J., and Noone, D.: Thunderstorms and upper troposphere chemistry during the early stages of the 2006 North American Monsoon, Atmospheric Chemistry and Physics, 12, 11,003-11,026, doi:10.5194/acp-12-11003-2012, 2012.

Beer, R.: Remote Sensing by Fourier Transform Spectrometry, Wiley, New York, 1992.

Bergamaschi, P., Frankenberg, C., Meirink, J. F., Krol, M., Dentener, F., Wagner, T., Platt, U., Kaplan, J. O., Körner, S., Heimann, M., and Dlugokencky, E. J.: Satellite chartography of atmospheric methane from SCIAMACHY on board ENVISAT: 2. Evaluation based on inverse model simulations, Journal of Geophysical Research-Atmospheres, 112 (D2), doi: 10.1029/2006jd007268, 2007.

Bergamaschi, P., Frankenberg, C., Meirink, J. F., Krol, M., Villani, M. G., Houweling, S., Dentener, F., Dlugokencky, E. J., Miller, J. B., Gatti, L. V., and Engel, A.: Inverse modeling of global and regional CH_4 emissions using SCIAMACHY satellite retrievals, Journal of Geophysical Research-Atmospheres, 114 (D22), doi:10.1029/2009jd012287, 2009.

Bian, H., Chin, M., Kawa, S. R., Yu, H., Diehl, T., and Kucsera, T.: Multiscale carbon monoxide and aerosol correlations from satellite measurements and the GOCART model: Implication for emissions and atmospheric atmospheric evolution, Journal of Geophysical Research-Atmospheres, 115 (D7), doi:10.1029/2009jd012781, 2010.

Bloom, A. A., Worden, J., Jiang, Z., Worden, H., Kurosu, T., Frankenberg, C., and Schimel, D.: Remote-sensing constraints on South America fire traits by Bayesian fusion of atmospheric and surface data, Geophysical Research Letters, 42 (4), doi:10.1002/2014GL062584, 2015.

Bohren, C. F. and Huffman, D. R.: Absorption and Scattering of Light by Small Particles, John Wiley and Sons, New York, 1983.

Bousserez, N., Henze, D. K., Rooney, B., Perkins, A., Wecht, K. J., Turner, A. J., Natraj, V., and Worden, J. R.: Constraints on methane emissions in North America from future geostationary remote-sensing measurements, Atmospheric Chemistry and Physics, 16, 6175–6190, doi:10.5194/acp-16- 6175-2016, 2016.

Breul, H. and Doman, L.: U.S. Expected to be Largest Producer of Petroleum and Natural Gas Hydrocarbons in 2013, Today in Energy, http://www.eia.gov/todayinenergy/detail.cfm?id=13251, 2013.

Brown, M.G., Baker, J., Colonero, C., Costa, J., Gardner, T., Kelly. M., Schultz, K., Tyrrell, B., and Wey, J.: Digital-pixel focal plane array development, Proc. SPIE 7608, Quantum Sensing and Nanophotonic Devices VII, 76082H (January 22, 2010); doi:10.1117/12.838314, 2010.

Brunekreef, B. and Holgate, S. T.: Air pollution and health, The Lancet, 360 (9341), 1233–1242, doi: 10.1016/s0140-6736(02)11274-8, 2002.

Butz, A., Galli, A., Hasekamp, O., Landgraf, J., Tol, P., and Aben, I.: TROPOMI aboard Precursor Sentinel-5 Precursor: Prospective performance of CH_4 retrievals for aerosol and cirrus loaded atmospheres, Remote Sensing of Environment, 120, 267–276, DOI:10.1016/j.rse.2011.05.030, 2012.

Ciais, P., Sabine, C., Bala, G., Bopp, L., Brovkin, V., Canadell, J., Chhabra, A., DeFries, R., Galloway, J., Heimann, M., Jones, C., Le Qu éré, C., Myneni, R. B., Piao S., and Thornton P.: Carbon and Other Biogeochemical Cycles, in: Climate Change 2013: The Physical Science Basis. Contribution of Working Group I to the Fifth Assessment Report of the Intergovernmental Panel on Climate Change [Stocker, T. F., Qin, D., Plattner, G.-K., Tignor, M., Allen, S. K., Bosc Hung, J., Nauels, A., Xia, Y., Bex, B., and Midgley, P. M. (Eds.)]. Cambridge University Press, Cambridge, United Kingdom and New York, NY, USA, 465–570, doi:10.1017/ CBO9781107415324.015, 2013.

CEOS: A Geostationary Satellite Constellation for Observing Global Air Quality: An International Path Forward, available at http://ceos.org/document_management/Virtual_Constellations/ACC/Documents/ACC_White-Paper-A-Geostationary-Satellite-Cx-for-Observing-Global-AQ-v4_Apr2011.pdf, 2011.

Clerbaux, C., Boynard, A., Clarisse, L., George, M., Hadji-Lazaro, J., Herbin, H., Hurtmans, D., Pommier, M., Razavi, A., Turquety, S., Wespes, C., and Coheur, P.-F.: Monitoring of atmospheric composition using the thermal infrared IASI/MetOp sounder, Atmospheric Chemistry and Physics, 9, 6041–6045, 2009.

Conley, S., Franco, G., Faloona, I., Blake, D. R., Peischl, J., and Ryerson, T. B.: Methane emissions from the 2015 Aliso Canyon blowout in Los Angeles, CA, Science, doi: 10.1126/science.aaf, 2348, 2016.

Crevoisier, C., Clerbaux, C., Guidard, V., Phulpin, T., Armante, R., Barret, B., Camy-Peyret, C.,Chaboureau, J.-P., Coheur, P.-F., Crépeau, L., Dufour, G., Labonnote, L., Lavanant, L., Hadji- Lazaro, J., Herbin, H., Jacquinet-Husson, N., Payan, S., Péquignot, E., Pierangelo, C., Sellitto, P., and Stubenrauch, C.: Towards IASI-New Generation (IASI-NG): impact of improved spectral resolution and radiometric noise on the retrieval of thermodynamic, chemistry and climate variables, Atmospheric Measurement Techniques, 7, 4367–4385, doi:10.5194/amt-7-4367-2014, 2014.

Deeter, M. N., Emmons, L. K., Edwards, D. P., Gille, J. C., and Drummond, J. R.: Vertical resolution and information content of CO profiles retrieved by MOPITT, Geophysical Research Letters, 31, 15112, doi:10.1029/2004GL020235, 2004.

Deeter, M. N., Edwards, D. P., Gille, J. C., and Drummond, J. R.: CO retrievals based on MOPITT near-infrared observations, Journal of Geophysical Research-Atmospheres, 114 (D4), doi:10.1029/2008JD010872, 2009.

Deeter, M. N., Worden, H. M., Gille, J. C., Edwards, D. P., Mao, D., and Drummond, J. R.: MOPITT multispectral CO retrievals: Origins and effects of geophysical radiance errors, Journal of Geophysical Research-Atmospheres, 116 (D15), doi:10.1029/2011JD015703, 2011.

Deeter, M. N., Martínez-Alonso, S., Edwards, D. P., Emmons, L. K., Gille, J. C., Worden, H. M., Pittman, J. V., Daube, B. C., and Wofsy, S. C.: Validation of MOPITT Version 5 thermal-infrared, near-infrared, and multispectral carbon monoxide profile retrievals for 2000–2011, Journal of Geophysical Research-Atmospheres, 118 (12), 6710–6725, doi:10.1002/jgrd.50272, 2013.

Drummond, J. R., Zou, J., Nichitiu, F., Kar, J., Deschambaut, R., and Hackett, J.: A review of 9-year performance and operation of the MOPITT instrument, Advances in Space Research, 45 (6), 760–774, doi:10.1016/j.asr.2009.11.019, 2010.

Edwards, D. P., Halvorson, C. M., and Gille, J. C.: Radiative transfer modeling for the EOS Terra satellite Measurement of Pollution in the Troposphere (MOPITT) instrument, Journal of Geophysical Research-Atmospheres, 104 (D14), 16755–16775, doi:10.1029/1999JD900167, 1999.

Edwards, D. P., Emmons, L. K., Hauglustaine, D. A., Chu, D. A., Gille, J. C., Kaufman, Y. J., Pétron, G., Yurganov, L. N., Giglio, L., Deeter, M. N., and Yudin, V.: Observations of carbon monoxide and aerosols from the Terra satellite: Northern Hemisphere variability, Journal of Geophysical Research-Atmospheres, 109 (D24), doi:10.1029/2004jd004727, 2004.

Edwards, D. P., Arellano, A. F., and Deeter, M. N.: A satellite observation system simulation experiment for carbon monoxide in the lowermost troposphere, Journal of Geophysical Research-Atmospheres, 114 (D14), doi:10.1029/2008JD011375, 2009.

Emmons, L. K., Edwards, D. P., Deeter, M. N., Gille, J. C., Campos, T., Nédélec, P., Novelli, P., and Sachse, G.: Measurements of Pollution In The Troposphere (MOPITT) validation through 2006, Atmospheric Chemistry and Physics, 9, 1795–1803, doi.org/10.5194/acp-9-1795-2009, 2009.

Fann, N., Lamson, A. D., Anenberg, S. C., Wesson, K., Risley, D., and Hubbell, B. J.: Estimating the National Public Health Burden Associated with Exposure to Ambient PM2.5 and Ozone, Risk Analysis, 32 (1), 81–95, doi: 10.1111/j.1539-6924.2011.01630.x, 2012.

Fisher, J. A., Jacob, D. J., Purdy, M. T., Kopacz, M., Le Sager, P., Carouge, C. C., Holmes, C. D., Yantosca, R. M., Batchelor, R. L., Strong, K., and Diskin, G.S.: Source attribution and interannual variability of Arctic pollution in spring constrained by aircraft (ARCTAS, ARCPAC) and satellite (AIRS) observations of carbon monoxide, Atmospheric Chemistry and Physics, 10 (3), 977–996, doi.org/10.5194/acp-10-977-2010, 2010.

Fishman, J., Iraci, L. T., Al-Saadi, J., Chance, K., Chavez, F., Chin, M., Coble, P., Davis, C., DiGiacomo, P. M., Edwards, D., Eldering, A., Goes, J., Herman, J., Hu, C., Jacob, D. J., Jordan, C., Kawa, S. R., Key, R., Liu, X., Lohrenz, S., Mannino, A., Natraj, V., Neil, D., Neu, J.,

Newchurch, M., Pickering, K., Salisbury, J., Sosik, H., Subramaniam, A., Tzortziou, M., Wang, J., and Wang, M.: The United States' Next Generation of Atmospheric Composition and Coastal Ecosystem Measurements: NASA's Geostationary Coastal and Air Pollution Events (GEO-CAPE) Mission, Bulletin of the American Meteorological Society, 93 (10), 1547–1566, doi: 10.1175/bams-d-11-00201.1, 2012.

Flynn, L., Long, C., Wu, X., Evans, R., Beck, C.T., Petropavlovskikh, I., McConville, G., Yu, W., Zhang, Z., Niu, J., and Beach, E.: Performance of the Ozone Mapping and Profiler Suite (OMPS) products, Journal of Geophysical Research-Atmospheres, 119, 6181–6195, doi:10.1002/2013JD020467, 2014.

Flynn, C. M., Pickering, K. E., Crawford, J. H., Weinheimer, A. J., Diskinc, G., Thornhill, K. L., Loughnerb, C., Pius Lee, and Strode, S. A.: Variability of O3 and NO2 profile shapes during DISCOVER-AQ: Implications for satellite observations and comparisons to model-simulated profiles. Atmospheric Environment, 147, 133–156, doi:10.1016/j.atmosenv.2016.09.068, 2016.

Fortems-Cheiney, A., Chevallier, F., Pison, I., Bousquet, P., Szopa, S., Deeter, M. N., and Clerbaux, C.: Ten years of CO emissions as seen from Measurements of Pollution in the Troposphere (MOPITT), Journal of Geophysical Research-Atmospheres, 116 (D5), doi:10.1029/2010JD014416., 2011.

Frankenberg, C., Meirink, J. F., van Weele, M., Platt, U., and Wagner, T.: Assessing Methane Emissions from Global Space-Borne Observations, Science, 308 (5724), 1010–1014, doi:10.1126/science.1106644, 2005.

Frankenberg, C., Aben, I., Bergamaschi, P., Dlugokencky, E. J., van Hees, R., Houweling, S., van der Meer, P., Snel, R., and Tol, P.: Global column averaged methane mixing ratios from 2003 to 2009 as derived from SCIAMACHY: Trends and variability, Journal of Geophysical Research-Atmospheres, 116 (D4), doi:10.1029/2010JD014849, 2011.

GMES-GAS: Global Monitoring for Environment and Security Atmosphere Core Service (GACS), in Implementation Group – Final Report, available at: http://www.gmes.info/pages-principales/library/implementation-groups/gmes-atmosphere-core-service/ , 2009.

Galmarini, S., Koffi, B., Solazzo, E., Keating, T., Hogrefe, C., Schulz, M., Benedictow, A., Griesfeller, J. J., Janssens-Maenhout, G., Carmichael, G., and Fu, J.: Technical note: Coordination and harmonization of the multi-scale, multi-model activities HTAP2, AQMEII3, and MICS-Asia3: simulations, emission inventories, boundary conditions, and model output formats., Atmospheric Chemistry and Physics, 17 (2), 1543–1555, 2017.

Gambacorta, A., Barnet, C., Wolf, W., King, T., Maddy, E., Strow, L., Xiong, X., Nalli, N., and Goldberg, M.: An Experiment Using High Spectral Resolution CrIS Measurements for Atmospheric Trace Gases: Carbon Monoxide Retrieval Impact Study, IEEE Geoscience and Remote Sensing Letters, 11 (9), 1639–1643, 2014.

Garnett, J. D., Farris, M. C., Wong, S. S., Zandian, M., Hall, D. N., Jacobson, S., Luppino, G., Parker, S., Dorn, D., Franka, S., and Freymiller, E.: 2Kx2K molecular beam epitaxy HgCdTe detectors for the James Webb Space Telescope NIRCam instrument, in: Proceedings of SPIE, 5499, 35-46, 2004.

Gaubert, B., Arellano, A. F., Barré, J., Worden, H. M., Emmons, L. K., Tilmes, S., Buchholz, R. R., Vitt, F., Raeder, K., Collins, N., and Anderson, J. L.: Toward a chemical reanalysis in a coupled chemistry-climate model: An evaluation of MOPITT CO assimilation and its impact on tropospheric composition, Journal of Geophysical Research-Atmospheres, 121 (12), 7310–7343, doi:10.1002/2016JD024863, 2016.

George, M., Clerbaux, C., Hurtmans, D., Turquety, S., Coheur, P.-F., Pommier, M., Hadji-Lazaro, J., Edwards, D. P., Worden, H., Luo, M., Rinsland, C., and McMillan, W.: Carbon monoxide distributions from the IASI/METOP mission: evaluation with other spaceborne remote sensors, Atmospheric Chemistry and Physics, 9, 8317–8330, 2009.

Gloudemans, A. M. S., Schrijver, H., Hasekamp, O. P., and Aben, I.: Error analysis for CO and CH_4 total column retrievals from SCIAMACHY 2.3μm spectra, Atmospheric Chemistry and Physics, 8, 3999–4017, 2008.

Green, R. O., Pieters, C., Mouroulis, P., Eastwood, M., Boardman, J., Glavich, T., Isaacson, P., Annadurai, M., Besse, S., Barr, D., and Buratti, B.: The Moon Mineralogy Mapper (M^3) imaging spectrometer for lunar science: Instrument description, calibration, on-orbit

measurements, science data calibration and on-orbit validation, Journal of Geophysical Research-Planets, 116 (E10), doi:10.1029/2011JE003797, 2011.

Grell, G., Peckham, S., Schmitz, R., McKeen, S., Frost, G., Skamarock, W., and Eder, B.: Fully coupled "online" chemistry within the WRF model, Atmospheric Environment, 39 (37), 6957–6975, doi:10.1016/j.atmosenv.2005.04.027, 2005.

Guizar-Sicairos, M., Thurman, S. T., and Fienup, J. R.: Efficient subpixel image registration algorithms, Optics Letters, 33 (2), 156–158, doi:10.1364/ol.33.000156, 2008.

He, H., Stehr, J. W., Hains, J. C., Krask, D. J., Doddridge, B. G., Vinnikov, K. Y., Canty, T. P., Hosley, K. M., Salawitch, R. J., Worden, H. M., and Dickerson, R. R.: Trends in emissions and concentrations of air pollutants in the lower troposphere in the Baltimore/Washington airshed from 1997 to 2011, Atmospheric Chemistry and Physics, 13 (15), 7859–7874, doi:10.5194/acp-13-7859-2013, 2013.

Heidinger, A.: ABI Cloud Mask Algorithm Theoretical Basis Document, NOAA, 2011. http://www.goes-r.gov/products/ATBDs/baseline/Cloud_CldMask_v2.0_no_color.pdf, last access: 6 October 2016, 2011.

Hess, M., Koepke, P., and Schult, I.: Optical properties of aerosols and clouds: The software package OPAC, Bulletin of the American meteorological society, 79 (5), 831–844, 1998.

Holloway, T., Levy, H., and Kasibhatla, P.: Global distribution of carbon monoxide, Journal of Geophysical Research-Atmospheres, 105 (D10), 12123–12147, doi:10.1029/1999JD901173, 2000.

Howard, T., Ferrara, T. W., and Townsend-Small, A.: Sensor transition failure in the high flow sampler: Implications for methane emission inventories of natural gas infrastructure, Journal of the Air & Waste Management Association, doi:10.1080/10962247.2015.1025925, 2015.

Huang, M., Bowman, K. W., Carmichael, G. R., Pierce, R. B., Worden, H. M., Luo, M., Cooper, R., Pollack, I. B., Ryerson, T. B., and Brown, S. S.: Impact of Southern California anthropogenic emissions on ozone pollution in the mountain states: Model analysis and observational evidence from space, Journal of Geophysical Research-Atmospheres, 118, doi:10.1002/2013JD020205, 2013.

Hudman, R. C., Murray, L. T., Jacob, D. J., Millet, D. B., Turquety, S., Wu, S., Blake, D. R., Goldstein, A. H., Holloway, J., and Sachse, G. W.: Biogenic versus anthropogenic sources of CO in the United States, Geophysical Research Letters, 35 (4), doi:10.1029/2007gl032393, 2008.

IGACO, 2004: The changing atmosphere: An Integrated Global Atmospheric Chemistry Observation theme for the IGOS partnership. ESA SP-1282, GAW Rep. 159, WMO TD-1235, 72 pp. [https://library.wmo.int/pmb_ged/wmo-td_1235.pdf, accessed 10/12/2017]

Ingmann, P., Veihelmann, B., Langen, J., Lamarre, D., Stark, H., and Courrèges-Lacoste, G. B.: Requirements for the GMES Atmosphere Service and ESA's implementation concept: Sentinels-4/-5 and-5p, Remote sensing of environment, 120, 58–69, 2012.

Jacob, D. J., Turner, A. J., Maasakkers, J. D., Sheng, J., Sun, K., Liu, X., Chance, K., Aben, I., McKeever, J., and Frankenberg, C.: Satellite observations of atmospheric methane and their value for quantifying methane emissions, Atmospheric Chemistry and Physics, 16 (22), 14371–14396, doi: 10.5194/acp-2016-555, 2016.

Jiang, Z., Jones, D. B. A., Worden, J., Worden, H. M., Henze, D. K., and Wang, Y. X.: Regional data assimilation of multi-spectral MOPITT observations of CO over North America, Atmospheric Chemistry and Physics, 15 (12), 6801–6814, doi:10.5194/acp-15-6801-2015, 2015.

Jiang, Z., Jones, D. B. A., Worden, H. M., Deeter, M. N., Henze, D. K., Worden, J., Bowman, K. W., Brenninkmeijer, C. A. M., and Schuck, T. J.: Impact of model errors in convective transport on CO source estimates inferred from MOPITT CO retrievals, Journal of Geophysical Research-Atmospheres, 118 (4), 2073–2083, doi:10.1002/jgrd.50216, 2013.

Karion, A., Sweeney, C., Pétron, G., Frost, G., Hardesty, R. M., Kofler, J., Miller, B. R., Newberger, T., Wolter, S., Banta, R., Brewer, A., Dlugokencky, E., Lang, P., Montzka, S. A., Schnell, R., Tans, P., Trainer, M., Zamora, R., and Conley, S.: Methane emissions estimate from airborne measurements over a western United States natural gas field, Geophysical Research Letters, 40 (16), 4393–4397, DOI:10.1002/grl.50811, 2013.

Katzenstein, A. S., Doezema, L. A., Simpson, I. J., Blake, D. R., and Rowland, F. S.: Extensive regional atmospheric hydrocarbon pollution in the southwestern United States, Proceedings

of the National Academy of Sciences of the United States of America, 100 (21), 11975–11979, doi:10.1073/pnas.1635258100, 2003.

Kopacz, M., Jacob, D. J., Henze, D. K., Heald, C. L., Streets, D. G., and Zhang, Q.: Comparison of adjoint and analytical Bayesian inversion methods for constraining Asian sources of carbon monoxide using satellite (MOPITT) measurements of CO columns. Journal of Geophysical Research-Atmospheres, 114 (D4), 1–10, 2009.

Kopacz, M., Jacob, D. J., Henze, D. K., Heald, C. L., Streets, D. G., and Zhang, Q.: Global estimates of CO sources with high resolution by adjoint inversion of multiple satellite datasets (MOPITT, AIRS, SCIAMACHY, TES), Atmospheric Chemistry and Physics, 10 (3), 855–876, doi: 10.5194/acp-10-855-2010, 2010.

Kort, E. A., Eluszkiewicz, J., Stephens, B. B., Miller, J. B., Gerbig, C., Nehrkorn, T., Daube, B. C., Kaplan, J. O., Houweling, S., and Wofsy, S. C.: Emissions of CH_4 and N_2O over the United States and Canada based on a receptor-oriented modeling framework and COBRA-NA atmospheric observations, Geophysical Research Letters, 35 (18), doi: 10.1029/2008gl034031, 2008.

Kumer, J. J. B., Rairden, R. L., Roche, A. E., Chevallier, F., Rayner, P. J., and Moore, B.: September. Progress in development of Tropospheric Infrared Mapping Spectrometers (TIMS): GeoCARB Greenhouse Gas (GHG) application. In Infrared Remote Sensing and Instrumentation XXI (Vol. 8867, p. 88670K). International Society for Optics and Photonics, 2013.

Lee, S., Hong, Y., Song, C. K., Lee, J., Choi, W. J., Kim, D., Moon, K. J., and Kim, J.: Plan of Korean Geostationary Environment Satellite over Asia- Pacific region, in: EGU General Assembly 2010, Vienna, Austria, 2010.

Levelt, P. F., van den Oord, G. H., Dobber, M. R., Malkki, A., Visser, H., de Vries, J., Stammes, P., Lundell, J. O., and Saari, H.: The ozone monitoring instrument, IEEE Transactions on Geoscience and Remote Sensing, 44 (5), 1093–1101, doi: 10.1109/TGRS.2006.872333, 2006.

Levi, A, Simonds, J., and Gruber, C.: CHIRP Technology Demonstration Project, in: AIAA Space 2011 Conference and Exposition, doi:10.2514/6.2011-7333, 2011

Loomis, D., Grosse, Y., Lauby-Secretan, B., El Ghissassi, F., Bouvard, V., Benbrahim-Tallaa, L., Guha, N., Baan, R., Mattock, H., and Straif, K.: The carcinogenicity of outdoor air pollution, Lancet Oncology, 14 (13), 1262–1263, doi:10.1016/s1470-2045(13)70487-X, 2013.

Ludwig, C. B., Malkmus, W., Griggs, M., and Bartle, E. R.: Monitoring of Air Pollution by Satellites (MAPS), Phase 1, NASA-CR-112137, GDCA-HAB73-005, 1973.

Malley, C. S., Kuylenstierna, J. C., Vallack, H. W., Henze, D. K., Blencowe, H., and Ashmore, M. R.: Preterm birth associated with maternal fine particulate matter exposure: A global, regional and national assessment, Environment International, available at: https://doi.org/10.1016/j.envint.2017.01.023 , 2017.

Massie, S. T., Gille, J. C., Edwards, D. P., and Nandi, S.: Satellite observations of aerosol and CO over Mexico City, Atmospheric Environment, 40 (31), 6019–6031, doi:10.1016/j.atmosenv.2005.11.065, 2006.

Matsunaga, T., Maksyutov, S., Morino, I., Yoshida, Y., Saito, M., Noda, H., Kamei, A., Kawazoe, F., and Yokot, T.: Recent Progress in NIES GOSAT and GOSAT-2 Projects, presented at 13 th International Workshop on Greenhouse Gas Measurements from Space, Helsinki, Finland, June 6 – 8, available at: http://iwggms13.fmi.fi/presentations/j06_s01_02_Matsunaga.pdf, 2017.

Meirink, J. F., Bergamaschi, P., Frankenberg, C., d'Amelio, M. T., Dlugokencky, E. J., Gatti, L. V., Houweling, S., Miller, J. B., Röckmann, T., Villani, M. G., and Krol, M. C.: Four-dimensional variational data assimilation for inverse modeling of atmospheric methane emissions: Analysis of SCIAMACHY observations, Journal of Geophysical Research-Atmospheres, 113 (D17), doi: 10.1029/2007jd009740, 2008.

Miller, S. M., Matross, D. M., Andrews, A. E., Millet, D. B., Longo, M., Gottlieb, E. W., Hirsch, A. I., Gerbig, C., Lin, J. C., Daube, B. C., and Hudman, R. C.: Sources of carbon monoxide and formaldehyde in North America determined from high-resolution atmospheric data, Atmospheric Chemistry and Physics, 8 (3), 7673–7696, doi: 10.5194/acp-8-7673-2008, 2008.

Miller, S. M., Wofsy, S. C., Michalak, A. M., Kort, E. A., Andrews, A. E., Biraud, S. C., Dlugokencky, E. J., Eluszkiewicz, J., Fischer, M. L., Janssens-Maenhout, G., Miller, B. R., Miller, J. B., Montzka, S. A., Nehrkorn, T., and Sweeney, C.: Anthropogenic emissions of

methane in the United States, Proceedings of the National Academy of Sciences of the United States, 110 (50), 20018–20022, doi:10.1073/pnas.1314392110, 2013.

Morino, I., Uchino, O., Inoue, M., Yoshida, Y., Yokota, T., Wennberg, P., Toon, G. C., Wunch, D., Roehl, C. M., Notholt, J., and Warneke, T.: Preliminary validation of column-averaged volume mixing ratios of carbon dioxide and methane retrieved from GOSAT short-wavelength infrared spectra, Atmospheric Measurement Techniques, 4, 1061–1076, doi:10.5194/amt-4-1061-2011, 2011.

Myhre, G., Shindell, D., Bréon, F. M., Collins, W., Fuglestvedt, J., Huang, J., Koch, D., Lamarque, J. F., Lee, D., Mendoza, B., and Nakajima, T.: Anthropogenic and Natural Radiative Forcing. The Physical Science Basis. Contribution of Working Group I to the Fifth Assessment Report of the Intergovernmental Panel on Climate Change 2013, Cambridge University Press, Cambridge, United Kingdom and New York, USA, available at: http://www.ipcc.ch/pdf/assessment- report/ar5/wg1/WG1AR5_Chapter08_FINAL.pdf, 2013.

National Academies of Sciences, Engineering, and Medicine: Powering Science: NASA's Large Strategic Science Missions. Washington, DC: The National Academies Press. https://doi.org/10.17226/24857 , p33, p81, 2017.

National Research Council: Earth science and applications from space: national imperatives for the next decade and beyond, The National Academies Press, Washington, D.C., available at: https://doi.org/10.17226/11820, 2007.

National Research Council: Air Quality Management in the United States, The National Academies Press, Washington, D.C., doi:10.17226/10728, 2004.

Nédélec P., Blot R., Boulanger D., Athier, G., Cousin, J-M., Gautron, B., Petzold, A., Volz-Thomas, A., and Thouret, V.: Instrumentation on commercial aircraft for monitoring the atmospheric composition on a global scale: the IAGOS system, technical overview of ozone and carbon monoxide measurements, MOZAIC-IAGOS special issue, Tellus B, 67, 27791, http://dx.doi.org/10.3402./tellusb.v67.27791, 2015.

Neil, D. O., Gordley, L. L., Marshall, B. T., and Sachse, G. W.: Tropospheric carbon monoxide measurements from geostationary orbit, in: Europto Remote Sensing, 265–273, International Society for Optics and Photonics, 2001.

O'Brien, D. M., Polonsky, I. N., Utembe, S. R., and Rayner, P. J.: Potential of a geostationary geoCARB mission to estimate surface emissions of CO_2, CH_4 and CO in a polluted urban environment: case study Shanghai, Atmospheric Measurement Techniques, 9, 4633–4654, https://doi.org/10.5194/amt-9-4633-2016, 2016.

O'Dell, C. W., Connor, B., Bösch, H., O'Brien, D., Frankenberg, C., Castano, R., Christi, M., Eldering, D., Fisher, B., Gunson, M., McDuffie, J., Miller, C. E., Natraj, V., Oyafuso, F., Polonsky, I., Smyth, M., Taylor, T., Toon, G. C., Wennberg, P. O., and Wunch, D.: The ACOS CO_2 retrieval algorithm – Part 1: Description and validation against synthetic observations, Atmospheric Measurement Techniques, 5, 99–121, https://doi.org/10.5194/amt-5-99-2012, 2012.

Palmer, P. I., Suntharalingam, P., Jones, D., Jacob, D. J., Streets, D. G., Fu, Q., Vay, S. A., and Sachse, G. W.: Using CO_2: CO correlations to improve inverse analyses of carbon fluxes, Journal of Geophysical Research-Atmospheres, 111 (D12), doi:10.1029/2005jd006697, 2006.

Pan, L., Edwards, D. P., Gille, J. C., Smith, M. W., and Drummond, J. R.: Satellite remote sensing of tropospheric CO and CH_4: forward model studies of the MOPITT instrument, Applied Optics, 34(30), 6976–6988, doi:10.1364/AO.34.006976, 1995.

Payne, V. H., Clough, S. A., Shephard, M. W., Nassar, R., and Logan, J. A.: Information-centered representation of retrievals with limited degrees of freedom for signal: Application to methane from the Tropospheric Emission Spectrometer, Journal of Geophysical Research-Atmospheres, 114 (D10), doi:10.1029/2008JD010155, 2009.

Pechony, O., Shindell, D. T., and Faluvegi, G.: Direct top-down estimates of biomass burning CO emissions using TES and MOPITT versus bottom-up GFED inventory, Journal of Geophysical Research-Atmospheres, 118 (14), 8054–8066, doi:10.1002/jgrd.50624, 2013.

Pétron, G., Frost, G., Miller, B. R., Hirsch, A. I., Montzka, S. A., Karion, A., Trainer, M., Sweeney, C., Andrews, A. E., Miller, L., and Kofler, J.: Hydrocarbon emissions characterization in the

Colorado Front Range: A pilot study, Journal of Geophysical Research-Atmospheres, 117 (D4), doi:10.1029/2011jd016360, 2012.

Pfister, G., Gille, J. C., Ziskin, D., Francis, G., Edwards, D. P., Deeter, M. N., and Abbott, E.: Effects of a Spectral Surface Reflectance on Measurements of Backscattered Solar Radiation: Application to the MOPITT Methane Retrieval, Journal of Atmospheric and Oceanic Technology, 22 (5), 566–574, doi:10.1175/JTECH1721.1, 2005.

Pfister, G. G., Reddy, P., Barth, M. C., Flocke, F. F., Fried, A., Herndon, S. C., Sive, B. C., Sullivan, J. T., Thompson, A. M., Yacovitch, T. I., Weinheimer, A. J., and Wisthaler, A.: Using observations and source specific model tracers to characterize pollutant transport during FRAPPÉ and DISCOVER-AQ, Journal of Geophysical Research-Atmospheres, doi:10.1002/2017JD027257, 2017.

Pickett-Heaps, C. A., Jacob, D. J., Wecht, K. J., Kort, E. A., Wofsy, S. C., Diskin, G. S., Worthy, D. E. J., Kaplan, J. O., Bey, I., and Drevet, J.: Magnitude and seasonality of wetland methane emissions from the Hudson Bay Lowlands (Canada), Atmospheric Chemistry and Physics, 11, 3773–3779, doi:10.5194/acp-11-3773-2011, 2011

Polonsky, I. N., O'Brien, D. M., Kumer, J. B., and O'Dell, C. W.,: Performance of a geostationary mission, geoCARB, to measure CO_2, CH_4 and CO column-averaged concentrations. Atmospheric Measurement Techniques, 7(4), 959–981, 2014.

Reichle H. G., Jr., Anderson, B. E., Connors, V. S., Denkins, T., Forbes, D. A., Gormsen, B. B., Langenfelds, R. L., Neil, D. O., Nolf, S. R., Novelli, P. C., and Pougatchev, N. S.: Space shuttle based global CO measurements during April and October 1994, MAPS instrument, data reduction, and data validation, Journal of Geophysical Research-Atmospheres, 104 (D17), 21443–21454, 1999.

Rodgers, C. D., Wells, R. J., Grainger, R. G., Taylor, F. W.: Improved stratospheric and mesospheric sounder validation: General approach and in-flight radiometric calibration, Journal of Geophysical Research-Atmospheres, 101 (D6), 9775–9793, 1996.

Rodgers, C. D.: Inverse Methods for Atmospheric Sounding - Theory and Practice, Series on Atmospheric Oceanic and Planetary Physics, Vol. 2, World Scientific Publishing, Singapore, 2000.

Russell, J. M. III, Gordley, L. L., Park, J. H., Drayson, S. R., Hesketh, D. H., Cicerone, R. J., Tuck, A. F., Frederick, J. E., Harries, J. E., and Crutzen, P.: The Halogen Occultation Experiment, Journal of Geophysical Research-Atmospheres, 98 (D6), 10777–10797, 1993.

Russell, P. B., Livingston, J. M., Hignett, P., Kinne, S., Wong, J., Chien, A., Bergstrom, R., Durkee, P., and Hobbs, P.V.: Aerosol-induced radiative flux changes off the United States mid-Atlantic coast: Comparison of values calculated from sunphotometer and in situ data with those measured by airborne pyranometer, Journal of Geophysical Research-Atmospheres, 104 (D2), 2289–2307, 1999.

Schepers, D., Guerlet, S., Butz, A., Landgraf, J., Frankenberg, C., Hasekamp, O., Blavier, J.-F., Deutscher, N. M., Griffith, D. W. T., Hase, F., Kyro, E., Morino, I., Sherlock, V., Sussmann, R., and Aben, I.: Methane retrievals from Greenhouse Gases Observing Satellite (GOSAT) shortwave infrared measurements: Performance comparison of proxy and physics retrieval algorithms, Journal of Geophysical Research-Atmospheres 117 (D10), D10307, doi:10.1029/2012JD017549, 2012.

Schneising, O., Burrows, J. P., Dickerson, R. R., Buchwitz, M., Reuter, M., and Bovensmann, H.: Remote sensing of fugitive methane emissions from oil and gas production in North American tight geologic formations, Earth's Future, 2 (10), 548–558, doi:10.1002/2014ef000265, 2014.

Schwietzke, S., Sherwood, O. A., Bruhwiler, L. M., Miller, J. B., Etiope, G., Dlugokencky, E. J., Michel, S. E., Arling, V. A., Vaughn, B. H., White, J. W., and Tans, P. P.:Upward revision of global fossil fuel methane emissions based on isotope database, Nature, 538 (7623), 88–91, doi:10.1038/nature19797, 2016.

Silva, S. J., Arellano, A. F., and Worden, H. M.: Toward anthropogenic combustion emission constraints from space-based analysis of urban CO_2/CO sensitivity, Geophysical Research Letters, 40 (18), 4971–4976, doi:10.1002/grl.50954, 2013.

Shindell, D. T., Faluvegi, G., Shindell, D. T., Faluvegi, G., Koch, D. M., Schmidt, G. A., Unger, N., and Bauer, S. E.: Improved attribution of climate forcing to emissions, Science, 326 (5953), 716–718, doi:10.1126/science.1174760, 2009.

Simmons, A., Fellous, J. L., Ramaswamy, V., Trenberth, K., Asrar, G., Balmaseda, M., Burrows, J. P., Ciais, P., Drinkwater, M., Friedlingstein, P., and Gobron, N.: Observation and integrated

Earth-system science: A roadmap for 2016–2025, Advances in Space Research, 57 (10), 2037–2103, doi:10.1016/j.asr.2016.03.008, 2016.

Spurr, R. J. D.: VLIDORT: A linearized pseudo-spherical vector discrete ordinate radiative transfer code for forward model and retrieval studies in multilayer multiple scattering media, Journal of Quantitative Spectroscopy and Radiative Transfer, 102, 316–343, doi:10.1016/j.jqsrt.2006.05.005, 2006.

Tolton, B. T. and Drummond, J. R.: Characterization of the length-modulated radiometer, Applied Optics, 36 (22), 5409–5420, https://doi.org/10.1364/AO.36.005409, 1997.

Trasande, L., Malecha, P., and Attina, T. M.: Particulate matter exposure and preterm birth: estimates of US attributable burden and economic costs, Environmental Health Perspectives, 124 (12), 1913, http://dx.doi.org/10.1289/ehp.1510810, 2016.

Turner, A. J., Jacob, D. J., Wecht, K. J., Maasakkers, J. D., Lundgren, E., Andrews, A. E., Biraud,S. C., Boesch, H., Bowman, K. W., Deutscher, N. M., Dubey, M. K., Griffith, D. W. T., Hase, F., Kuze, A., Notholt, J., Ohyama, H., Parker, R., Payne, V. H., Sussmann, R., Sweeney, C., Velazco, V. A., Warneke, T., Wennberg, P. O., and Wunch, D.: Estimating global and North American methane emissions with high spatial resolution using GOSAT satellite data, Atmospheric Chemistry and Physics, 15, 7049–7069, doi:10.5194/acp-15-7049-2015, 2015.

Turner, M. C., Jerrett, M., Pope III, C.A., Krewski, D., Gapstur, S. M., Diver, W. R., Beckerman, B. S., Marshall, J. D., Su, J., Crouse, D. L., and Burnett, R. T.: Long-term ozone exposure and mortality in a large prospective study, American journal of respiratory and critical care medicine, 193 (10), 1134–1142, doi 10.1164/rccm.2015081633OC, 2015.

U.S.: Air Quality Criteria for Carbon Monoxide, U.S. Department of Health, Education, and Welfare, Public Health Service, National Air Pollution Control Administration, Publication No. AP-62, Washington , D.C., March 19, 1970.

UNEP: Near-term Climate Protection and Clean Air Benefits: Actions for Controlling Short-Lived Climate Forcers, United Nations Environment Programme (UNEP), Nairobi, Kenya, http://www.unep.org/publications/ebooks/SLCF/, 2011.

Veefkind, J. P., Aben, I., McMullan, K., Forster, H., de Vries, J., Otter, G., Claas, J., Eskes, H. J., de Haan, J. F., Kleipool, Q., van Weele, M., Hasekamp, O., Hoogeveen, R., Landgraf, J., Snel, R., Tol, P., Ingmann, P., Voors, R., Kruizinga, B., Vink, R., Visser, H., and Levelt, P. F.: TROPOMI on the ESA Sentinel-5 Precursor: A GMES mission for global observations of the atmospheric composition for climate, air quality and ozone layer applications, Remote Sensing of Environment, 120, 70–83, doi:10.1016/j.rse.2011.09.027, 2012.

Vey, S., Dietrich, R., Rülke, A., Fritsche, M., Steigenberger, P., and Rothacher, M.: Validation of Precipitable Water Vapor within the NCEP/DOE Reanalysis Using Global GPS Observations from One Decade, Journal of Climate 23 (7), 1675–1695, 2010.

Vijayaraghavan, K., Snell, H. E, and Seigneur, C.: Practical Aspects of Using Satellite Data in Air Quality Modeling, Environmental Science and Technology, 42 (22), 8187–8192, doi:10.1021/es7031339, 2008.

Warner, J. X., Gille, J. C., Edwards, D. P., Ziskin, D. C., Smith, M. W., Bailey, P. L., and Rokke, L.: Cloud Detection and Clearing for the Earth Observing System Terra Satellite Measurements of Pollution in the Troposphere (MOPITT) Experiment, Applied Optics, 40 (8), 1269–1284, doi:10.1364/AO.40.001269, 2001.

Wecht, K. J., Jacob, D. J., Sulprizio, M. P., Santoni, G. W., Wofsy, S. C., Parker, R., Bösch, H., and Worden, J.: Spatially resolving methane emissions in California: constraints from the CalNex aircraft campaign and from present (GOSAT, TES) and future (TROPOMI, geostationary) satellite observations, Atmospheric Chemistry and Physics, 14, 8173–8184, doi:10.5194/acp- 14-8173-2014, 2014 (a).

Wecht, K. J., Jacob, D. J., Frankenberg, C., Jiang, Z., and Blake, D. R.: Mapping of North American methane emissions with high spatial resolution by inversion of SCIAMACHY satellite data, Journal of Geophysical Research-Atmospheres, 119 (12), 7741–7756, doi:10.1002/2014JD021551, 2014 (b).

West, J. J., Fiore, A. M., Horowitz, L. W., and Mauzerall, D. L.: Global health benefits of mitigating ozone pollution with methane emission controls, Proceedings of the National Academy of Sciences of the United States of America, 103 (11), 3988–3993, doi:10.1073/pnas.0600201103, 2006.

Westerling, A. L., Hidalgo, H. G., Cayan, D. R., and Swetnam, T. W.: Warming and earlier spring increase western US forest wildfire activity, Science, 313 (5789), 940–943, doi:10.1126/science.1128834, 2006.

Worden, H. M., Deeter, M. N., Edwards, D. P., Gille, J. C., Drummond, J. R., and P. Nédélec: Observations of near-surface carbon monoxide from space using MOPITT multispectral retrievals, Journal of Geophysical Research-Atmospheres, 115 (D18), doi:10.1029/2010JD014242, 2010.

Worden, H. M., Cheng, Y., Pfister, G., Carmichael, G. R., Zhang, Q., Streets, D. G., Deeter, M., Edwards, D. P., Gille, J. C., and Worden, J. R.: Satellite-based estimates of reduced CO and CO_2 emissions due to traffic restrictions during the 2008 Beijing Olympics, Geophysical Research Letters, 39 (14), doi:10.1029/2012GL052395, 2012.

Worden, H. M., Deeter, M. N., Frankenberg, C., George, M., Nichitiu, F., Worden, J., Aben, I., Bowman, K. W., Clerbaux, C., Coheur, P. F. and De Laat, A. T. J.: Decadal record of satellite carbon monoxide observations, Atmospheric Chemistry and Physics, 13 (2), 837-850, doi:10.5194/acp-13-837-2013, 2013.

Worden, J., Wecht, K., Frankenberg, C., Alvarado, M., Bowman, K., Kort, E., Kulawik, S., Lee, M., Payne, V., and Worden, H.: CH_4 and CO distributions over tropical fires during October 2006 as observed by the Aura TES satellite instrument and modeled by GEOS-Chem, Atmospheric Chemistry and Physics, 13 (7), 3679–3692, doi:10.5194/acp-13-3679-2013, 2013.

Worden, J., Jiang, Z., Jones, D., Alvarado, M., Bowman, K., Frankenberg, C., Kort, E. A., Kulawik, S. S., Lee, M., Liu, J., and Payne, V.: El Niño, the 2006 Indonesian peat fires, and the distribution of atmospheric methane, Geophysical Research Letters, 40 (18), 4938–4943, doi: 10.1002/grl.50937, 2013.

Wunch, D., Toon, G. C., Wennberg, P. O., Wofsy, S. C., Stephens, R. S., Fischer, M. K., Uchino, O., Abshire, J., Bernath, P., Biraud, S. C., and Blavier, J. F.: Calibration of the Total Carbon Column Observing Network using aircraft profile data, Atmospheric Measurement Techniques, 3, 1351–1362, doi:10.5194/amt-3-1351-2010, 2010.

Xiao, Y., Logan, J. A., Jacob, D. J., Hudman, R. C., Yantosca, R., and Blake, D. R.,: Global budget of ethane and regional constraints on US sources, Journal of Geophysical Research-Atmospheres, 113 (D21), doi: 10.1029/2007jd009415, 2008.

Zhang, L., Jacob, D. J., Bowman, K. W., Logan, J. A., Turquety, S., Hudman, R. C., Li, Q., Beer, R., Worden, H. M., Worden, J. R., and Rinsland, C. P.: Ozone-CO correlations determined by the TES satellite instrument in continental outflow regions, Geophysical Research Letters, 33 (18), doi:10.1029/2006gl026399, 2006.

Zoogman, P., Jacob, D. J., Chance, K., Worden, H. M., Edwards, D. P., and Zhang, L.: Improved monitoring of surface ozone by joint assimilation of geostationary satellite observations of ozone and CO, Atmospheric Environment, 84 (0), 254-261, doi:10.1016/j.atmosenv.2013.11.048, 2014.

Zoogman, P., Liu, X., Suleiman, R. M., Pennington, W. F, Flittner, D. E., Al-Saadi, J. A., Hilton, B. B., Nicks, D. K., Newchurch, M. J., Carr, J. L., Janz, S. J., Andraschko, M. R., Arola, A., Baker, B. D., Canova, B. P., Chan Miller, C., Cohen, R. C., Davis, J. E., Dussault, M. E., Edwards, D. P., Fishman, J., González Abad, G., Grutter, M., Herman, J. R., Houck, J., Jacob, D. J., Joiner, J., Kerridge, B. J., Kim, J., Krotkov, N. A., Lamsal, L., Lif, C., Lindfors, A., Martin, R. V., McElroy, C. T., McLinden, C., Natraj, V., Neil, D. O., Nowlan, C. R., O'Sullivan, E. J., Palmer, P. I., Pierce, R. B., Pippin, M. R., Saiz-Lopez, A., Spurr, R. J. D., Szykman, J. J., Torres, O., Veefkind, J. P., Veihelmanna, B., Wang, H., Wang, J., Ghula, A., and Chance, K.: Tropospheric Emissions: Monitoring of Pollution (TEMPO), Journal of Quantitative Spectroscopy and Radiative Transfer, 186, 17–39, doi:10.1016/j.jqsrt.2016.05.008, 2017.